

8. $^{40}\text{Ar}/^{39}\text{Ar}$ SINGLE-CRYSTAL DATING OF DETRITAL MUSCOVITE AND K-FELDSPAR FROM LEG 116, SOUTHERN BENGAL FAN: IMPLICATIONS FOR THE UPLIFT AND EROSION OF THE HIMALAYAS¹

Peter Copeland,^{2,3} T. Mark Harrison,^{2,4} and Matthew T. Heizler^{2,4}

ABSTRACT

Detrital K-feldspars and muscovites from Ocean Drilling Program Leg 116 cores that have depositional ages from 0 to 18 Ma have been dated by the $^{40}\text{Ar}/^{39}\text{Ar}$ technique. Four to thirteen individual K-feldspars have been dated from seven stratigraphic levels, each of which have a very large range, up to 1660 Ma. At each level investigated, at least one K-feldspar yielded an age minimum which is, within uncertainty, identical to the age of deposition. One to twelve single muscovite crystals from each of six levels have also been studied. The range of muscovite ages is less than that of the K-feldspars and, with one exception, reveal only a 20-Ma spread in ages. As with the K-feldspars, each level investigated contains muscovites with mineral ages essentially identical to depositional ages. These results indicate that a significant portion of the material in the Bengal Fan is first-cycle detritus derived from the Himalayas. Therefore, the significant proportion of sediment deposited in the distal fan in the early to mid Miocene can be ascribed to a significant pulse of uplift and erosion in the collision zone. Moreover, these data indicate that during the entire Neogene, some portion of the Himalayan orogen was experiencing rapid erosion (\leq uplift). The lack of granulite facies rocks in the eastern Himalayas and Tibetan Plateau suggests that very rapid uplift must have been distributed in brief pulses in different places in the mountain belt. We suggest that the great majority of the crystals with young apparent ages have been derived from the southern slope of the Himalayas, predominantly from near the main central thrust zone. These data provide further evidence against tectonic models in which the Himalayas and Tibetan plateaus are uplifted either uniformly during the past 40 m.y. or mostly within the last 2 to 5 m.y.

INTRODUCTION

Determination of the timing and rates of vertical tectonic activities are fundamental to assessment of virtually all geophysical processes during orogeny. Although modern geodetic methods can precisely constrain recent movements in tectonically active regions, other approaches requiring geochronology, either direct or indirect, are needed to extract these important parameters from the geologic record. For example, isotopically based age studies of minerals from differing elevations can reveal apparent uplift rates (e.g., Wagner et al., 1977; Harrison et al., 1979) and, in certain cases, the age of the onset of erosion (e.g., Copeland et al., 1987a). However, these studies are usually limited to assessment of uplift relative to the earth's surface (unroofing) and may not record the onset of unroofing due to the thermal inertia of the overburden. In contrast, the stratigraphic record preserved in the Bengal Fan has the potential for yielding information about uplift and erosion of the Himalayas that can not easily be obtained from land-based studies. One objective of the drilling of Leg 116, located at the distal end of the Bengal Fan, was to investigate the relationships between the stratigraphy and sedimentology of the fan and the tectonics of the India-Asia collision. Although the recovered core from Site 718 contains thick sections of early and mid Miocene sediment (Cochran, Stow, et al., 1989) suggesting rapid erosion in the Himalayas at about this time, sedimentation at the distal portion

of the fan may not reflect tectonic activity in the source area 3000 km away but may rather be the result of redeposition of material from an older part of the fan. Our approach is to test this hypothesis as well as to determine the provenance age of these turbidites and relate this information to the tectonics of the Himalayas and southern Tibetan Plateau where substantial regional geochronology is now available (e.g., Kai, 1981; Ferrara et al., 1983; Copeland et al., 1987a, b; Maluski et al., 1988; Hubbard and Harrison, 1989). The $^{40}\text{Ar}/^{39}\text{Ar}$ dating method (see McDougall and Harrison, 1988) was used to date single crystals and aggregates of detrital K-feldspar and muscovites from several stratigraphic intervals of the core recovered from Leg 116. A companion study (Corrigan and Crowley, this volume) has dated apatites from these samples by the fission-track method, with similar goals in mind.

Various models have been proposed for the tectonic evolution of the Himalayas and Tibetan Plateau (e.g., Dewey and Burke, 1973; Powell and Conaghan, 1979; Powell, 1986; Zhao and Morgan, 1987). Our results place constraints on these models as they provide further information concerning the timing, rates, and periodicity of uplift and erosion resulting from the India-Asia collision.

ANALYTICAL METHODS

Samples used in this study are the same as those used by Corrigan and Crowley (this volume). Individual samples were obtained by combining coarse silt and coarser material over 100-m intervals to obtain sufficient apatites for their study. Samples are referred to by site number followed by the number of meters below the sea floor at which the interval began (e.g., 718-560). The fossils used to date the stratigraphic horizons at Sites 717 and 718 were not ideal for the task (Gartner, this volume). Two problems contribute to the uncertainty of these age assignments: (1) the lack of fossiliferous beds in some intervals made extrapolation from other depths necessary, and (2) the potential occurrence of trans-

¹ Cochran, J. R., Stow, D.A.V., et al., 1990. *Proc. ODP, Sci. Results*, 116: College Station, TX, U.S.A. (Ocean Drilling Program).

² Department of Geological Sciences, State University of New York at Albany, Albany, NY 12222, U.S.A.

³ Present address: Department of Geosciences, University of Houston, Houston, TX 77204-5503, U.S.A.

⁴ Present address: Department of Earth and Space Sciences, University of California, Los Angeles, Los Angeles, CA 90024, U.S.A.

Table 1. Stratigraphic age estimates for sampled intervals (in millions of years) based on calcareous nanofossils (Gartner, this volume).

Sample	Minimum	Middle	Maximum
717-0	0.0	0.3	0.7
717-120	0.4	0.8	1.9
717-220	1.9	2.7	3.6
717-420	5.2	5.8	6.6
717-520	6.2	7.0	7.8
718-290	7.5	8.4	9.0
717-720	8.7	9.3	9.9
718-560	10.8	11.4	12.2
718-660	11.8	13.8	15.8
718-760	15.4	16.1	16.8
718-860	16.4	16.8	18.0

ported fauna in these turbidites allows the possibility that depositional ages are overestimates. Unfortunately, the sampling method used here introduces additional uncertainty to the depositional age of any individual grain analyzed in this study as it is impossible to say from what point within the 100-m interval a grain originally came. For representing these data on our figures we have chosen to treat all grains from a particular interval as if they came from the midpoint of the interval, with an uncertainty that encompasses the uncertainties in the ages of the top and bottom of the interval; the uncertainties in the endpoints are asymmetric, so some of the midpoints do not appear in the center of the line. The midpoints and ranges of these estimates are given in Table 1.

From the light fraction ($\rho < 2.9$) of these samples, muscovite and K-feldspar were separated by standard heavy liquid and magnetic procedures. The separates were sieved to 45 to 100 mesh (335 to 59 μm) for K-feldspars and 18 to 100 mesh (1000 to 59 μm) for muscovites.

Approximately 100 mg of K-feldspar and 60 to 100 mg of muscovite were packed in tin foil and sealed in evacuated quartz tubes. Along with the unknowns, four flux monitors were placed in the tubes at 1.5-cm intervals. The flux monitor used was our intralaboratory standard, biotite Fe-mica (Govindajaru, 1978), which has an age of 307.3 Ma. The samples were irradiated for 60 hr in the Ford Nuclear Reactor, University of Michigan. Flux gradients in individual tubes ranged from 2.0% to 2.4%. Correction factors used to account for interfering nuclear reactions were $(^{37}\text{Ar}/^{39}\text{Ar})_{\text{Ca}} = 0.000751$, $(^{36}\text{Ar}/^{37}\text{Ar})_{\text{Ca}} = 0.00021$, and $(^{40}\text{Ar}/^{39}\text{Ar})_{\text{K}} = 0.036$.

Both multigrain separates and single crystals were analyzed in this study. Ar analysis of the bulk separates was done using an automated Nuclide 4.5-60-RSS mass spectrometer and heating samples in a double vacuum resistance furnace following the procedures of Harrison and Fitz Gerald (1986). The extraction blank in this system below 1200°C averaged $\sim 3 \times 10^{-14}$ moles ^{40}Ar during the course of these experiments. For single-crystal analysis, minerals were removed from the tin packages and individual crystals were selected under a binocular microscope. In general, the largest crystals available were selected. These crystals were then placed in a circular copper sample holder that had six 60° sectors to separate crystals from different samples. The samples were heated through a glass window using a continuous Ar laser (for another example of this technique see Dalrymple and Duffield, 1988). Monitoring of samples during heating was done using a binocular microscope mounted slightly off axis from the laser beam. Heating times were generally 30 to 60 s. The gas was purified using a SAES 10 l/s getter operated at 0.85 A. Total system blank was $\sim 1 \times 10^{-16}$ moles ^{40}Ar ($^{40}\text{Ar}/^{36}\text{Ar} = 265$) during the course of these experiments. Ar

isotopes from these single crystals were analyzed using an automated VG 1200S mass spectrometer.

Step heating was performed on bulk separates of K-feldspar from three levels and muscovite from five levels. Because of the ambiguous results from the bulk analysis and the clear potential for mixing of multiple populations of grains, we chose to analyze individual grains of K-feldspar and muscovite using the laser heating system from other stratigraphic levels. Sixty-eight K-feldspars from seven stratigraphic intervals and forty-nine muscovites from six stratigraphic intervals were analyzed. Eight to thirteen K-feldspars and one to twelve muscovites were analyzed from each interval. Depending on the size of the crystal, one to five steps were heated per sample. Generally, K-feldspars were heated in 2–4 steps whereas muscovites were fused in a single step (Table 3). In four of the levels in which single K-feldspars were analyzed and two of the levels in which single muscovites were analyzed approximately 20 mg were then fused on the Nuclide mass spectrometer to obtain a bulk average for these levels.

In all cases, uncertainties quoted for Ar isotope ages are at the one-sigma level. These uncertainties include the analytical error in the measurement as well as the uncertainty in the J factor, estimated at 1%.

RESULTS

Results of Ar isotope analysis on the step heating experiments on the multigrain K-feldspars and muscovites are given in Table 2; age spectra are shown in Figure 1. Where more than one heating step was performed on the single crystals of K-feldspar and muscovite, the resultant age spectrum is shown in Figures 2–9. Ar isotope results for the single-crystal analyses and the ~ 20 -mg total fusion analyses from these same levels are given in Tables 3 and 4, respectively.

The age spectra for the bulk K-feldspars from levels 717-0, 718-290, and 718-860 shown in Figure 1 are generally U-shaped, with the age minima and total fusion ages increasing with increasing stratigraphic age. The multigrain muscovite samples show both relatively flat and irregular age spectra. The general increase of both minimum ages and total fusion ages for both the multigrain K-feldspar and muscovite samples could be expected from a basin that has as its source an actively uplifting mountain belt. However, little tectonic information can be obtained from Figure 1.

We think the variations in the K-feldspar age spectra for the single-crystal samples are significant and not an artifact of the heating method. The range in age spectra types seen in these samples is similar to the range of spectra from conventionally heated, multigrain samples described in the literature, albeit with considerably less resolution. These types of spectra include flat (e.g., grain 484, Fig 5; grain 401, Fig. 6), U-shaped or saddle-shaped (e.g., grain 411, Fig 5), monotonically decreasing age (e.g., grain 308, Fig 4; grain 450, Fig. 7), monotonically increasing age (e.g., grain 321, Fig. 4; grain 445, Fig. 7), and increasing age up to a "plateau" (e.g., grain 466, Fig. 7; grain 356, Fig. 8). In these samples there exists no relationship between spectral shape and age (cf. grains 321 and 445). A flat age spectrum indicates rapid cooling with no variation in the initial (or trapped) Ar composition in the crystal. Age spectra with increasing ages (either monotonically, grain 445, or rising up to a plateau, grain 466) result from either slow cooling through the closure temperature(s) of the crystal or a reheating event producing episodic loss. In some cases it may be possible to distinguish between these possibilities from the shape of the age spectra (i.e., grain 470, Fig. 7, is suggestive of episodic loss) but in general the number of steps analyzed here does not provide sufficient resolution.

Table 2. $^{40}\text{Ar}/^{39}\text{Ar}$ step heating results from multigrain separates of muscovite and K-feldspar from samples at Sites 717 and 718.

Temp °C	$^{40}\text{Ar}/^{39}\text{Ar}$	$^{37}\text{Ar}/^{39}\text{Ar}$	$^{36}\text{Ar}/^{39}\text{Ar}$ (E-3)	^{39}Ar (E-13 mol)	% ^{39}Ar released	$^{40}\text{Ar}^*$ %	$^{40}\text{Ar}^*/^{39}\text{Ar}_K$	Age \pm 1 s.d. (Ma)
717-0 K-feldspar (J = 0.005314; wt. = 104.10 mg)								
450	313.4	0.0032	954.8	0.017	0.018	9.41	31.18	278.0 \pm 702
500	46.54	0.0142	21.72	0.617	0.696	85.2	40.09	350.2 \pm 3.2
550	11.23	0.0066	3.898	1.85	2.73	88.2	10.04	94.3 \pm 3.1
600	7.157	0.0049	1.437	3.18	6.23	92.4	6.697	63.4 \pm 1.0
650	5.428	0.0056	0.4151	5.20	11.9	96.1	5.270	50.1 \pm 0.3
690	4.060	0.0057	0.1245	3.10	15.4	97.4	3.987	38.0 \pm 0.4
730	4.111	0.0077	0.2028	5.03	20.9	96.3	4.016	38.3 \pm 0.2
770	3.807	0.0096	0.9865	3.19	24.4	89.2	3.480	33.2 \pm 0.8
810	3.648	0.0077	0.2649	7.12	32.2	95.8	3.535	33.8 \pm 0.2
860	3.639	0.0061	0.0917	7.21	40.1	97.2	3.577	34.2 \pm 0.2
910	3.733	0.0072	0.6812	7.56	48.5	92.7	3.496	33.4 \pm 0.3
960	4.180	0.0062	0.4548	8.74	58.1	95.2	4.010	38.3 \pm 0.3
1000	5.126	0.0052	0.3445	5.25	63.8	96.2	4.988	47.5 \pm 0.4
1030	6.013	0.0055	0.6122	6.52	71.0	95.7	5.797	55.0 \pm 0.7
1060	6.675	0.0064	0.4922	5.36	76.9	96.5	6.494	61.5 \pm 0.8
1100	7.324	0.0092	2.469	2.15	79.3	87.9	6.559	62.2 \pm 3.1
1130	8.101	0.0080	0.6257	3.40	83.0	96.2	7.881	74.4 \pm 0.7
1170	8.853	0.0067	1.402	3.33	86.7	94.0	8.403	49.2 \pm 0.7
1220	8.508	0.0034	0.8063	4.48	91.6	96.0	8.234	77.7 \pm 0.4
1550	9.216	0.0031	0.0982	7.65	100	98.9	9.151	86.1 \pm 0.2
total fusion age = 54.3								
717-290 K-feldspar (J = 0.005414; wt. = 105.09 mg)								
400	11647	2.141	10630	0.004	0.014	72.6	8520	6951 \pm 59.9
450	239.8	0.0159	140.0	0.105	0.337	81.8	198.4	1316 \pm 17.6
500	73.42	0.0092	17.40	0.428	1.66	92.1	68.25	567.3 \pm 4.0
550	24.07	0.0178	3.025	0.876	4.37	94.8	23.14	213.0 \pm 3.3
600	14.28	0.0200	0.5047	1.05	7.62	96.8	14.10	132.7 \pm 0.9
640	7.399	0.0179	1.076	0.771	10.0	90.5	7.047	67.5 \pm 3.2
670	5.542	0.0374	0.2948	0.967	13.0	92.6	5.421	52.2 \pm 1.3
700	5.813	0.0204	1.848	1.46	17.5	86.9	5.232	50.4 \pm 1.5
740	6.008	0.0207	1.169	2.56	25.4	91.9	5.628	54.1 \pm 2.0
780	5.552	0.0241	1.641	1.80	31.0	88.0	5.033	48.5 \pm 0.4
830	5.342	0.0275	1.233	2.31	38.2	90.3	4.944	47.7 \pm 0.6
880	4.324	0.0257	0.6496	2.36	45.5	92.1	4.098	39.6 \pm 2.5
930	4.436	0.0137	1.216	1.76	50.9	87.7	4.041	39.0 \pm 2.9
980	5.363	0.0140	0.8891	2.49	58.6	93.7	5.065	48.8 \pm 2.1
1040	6.551	0.0122	0.6439	2.35	65.9	94.7	6.326	60.7 \pm 0.4
1090	6.920	0.0061	1.605	2.06	72.2	09.7	6.410	61.5 \pm 2.6
1130	7.587	0.0129	1.355	1.97	78.3	92.4	7.151	68.5 \pm 3.9
1150	7.713	0.0193	0.6454	0.866	81.0	92.9	7.488	71.7 \pm 2.0
1170	7.557	0.0075	0.0000	1.12	84.5	97.6	7.634	73.1 \pm 5.3
1220	7.666	0.0006	0.0000	2.27	91.5	99.1	7.731	74.0 \pm 4.4
1350	10.16	0.0156	0.0376	2.24	98.4	98.3	10.11	96.2 \pm 0.1
1550	21.56	0.0056	4.479	0.510	100	91.2	20.20	187.3 \pm 4.9
total fusion age = 79.2								
718-860 K-feldspar (J = 0.005407; wt. = 107.15 mg)								
450	193.0	0.0096	138.9	0.566	1.17	78.5	151.9	1082 \pm 7.7
500	25.30	0.0056	7.052	0.849	2.92	90.4	23.18	213.0 \pm 3.7
550	16.26	0.0013	0.9948	1.70	6.44	96.9	15.93	149.1 \pm 1.3
600	13.37	0.0028	0.5727	2.93	12.5	97.7	13.17	124.1 \pm 1.6
650	11.39	0.0017	0.0567	3.92	20.6	98.9	11.34	107.4 \pm 0.2
690	11.67	0.0032	0.5020	2.55	25.9	97.4	11.49	108.7 \pm 0.5
730	12.84	0.0059	1.725	2.40	30.8	94.8	12.29	116.1 \pm 1.3
780	14.06	0.0036	1.033	2.31	35.6	96.7	13.72	129.1 \pm 1.5
830	14.63	0.0028	1.851	1.74	39.2	95.6	14.05	132.1 \pm 3.8
880	14.10	0.0051	2.391	1.59	42.5	93.5	13.36	125.8 \pm 1.9
930	13.91	0.0035	0.0600	3.06	48.8	99.7	13.96	131.3 \pm 4.6
980	14.52	0.0361	3.163	0.531	49.9	89.8	13.56	127.6 \pm 2.8
1030	16.60	0.0011	2.359	0.527	51.0	92.4	15.87	148.5 \pm 3.2
1080	18.79	0.0048	0.5491	5.38	62.1	98.7	18.60	172.9 \pm 0.5
1120	20.72	0.0011	0.510	2.73	67.7	99.6	20.75	191.8 \pm 1.8
1160	22.81	0.0278	0.0720	0.273	68.3	97.0	23.20	213.2 \pm 8.8
1200	25.91	0.0016	0.6069	14.5	98.2	99.1	25.69	234.7 \pm 0.5
1300	28.00	0.0040	1.250	0.337	98.9	97.7	27.60	250.9 \pm 5.5
1550	42.12	0.0335	5.170	0.525	100	95.9	40.56	357.7 \pm 10.1
total fusion age = 182.7								
718-860 muscovite (J = 0.005265; wt. = 61.05 mg)								
650	31.98	1.456	66.06	2.96	6.49	39.1	12.52	115.2 \pm 1.0
740	15.08	0.1076	16.72	5.51	18.6	67.0	10.11	93.5 \pm 0.7
790	6.729	0.0061	3.453	10.8	42.2	84.2	5.673	53.1 \pm 1.1
850	7.700	0.0058	4.838	13.1	70.9	80.9	6.235	58.3 \pm 0.3

Table 2 (continued).

Temp °C	$^{40}\text{Ar}/^{39}\text{Ar}$	$^{37}\text{Ar}/^{39}\text{Ar}$	$^{36}\text{Ar}/^{39}\text{Ar}$ (E-3)	^{39}Ar (E-13 mol)	% ^{39}Ar released	$^{40}\text{Ar}^*$ %	$^{40}\text{Ar}^*/^{39}\text{Ar}_K$	Age \pm 1 s.d. (Ma)
910	8.356	0.0086	1.361	8.85	90.3	94.6	7.919	73.7 \pm 0.4
970	9.396	0.0119	0.7689	0.947	92.3	96.1	9.134	84.7 \pm 1.2
1030	7.748	0.0076	2.216	2.59	98.0	90.6	7.057	65.8 \pm 1.3
1100	10.25	0.0141	1.145	0.894	100	95.3	9.876	91.5 \pm 1.6
total fusion age = 69.6								
717-0 muscovite (J = 0.005387; wt. = 103.76 mg)								
650	18.11	0.0136	44.64	1.74	1.40	26.9	4.883	46.8 \pm 2.3
740	5.398	0.0043	10.64	6.63	6.77	41.0	2.217	21.4 \pm 0.5
800	2.568	0.0013	1.887	26.7	28.4	76.8	1.974	19.1 \pm 0.1
860	3.455	0.0013	3.216	47.2	66.6	71.4	2.469	23.8 \pm 0.1
920	3.556	0.0027	3.012	12.5	76.6	73.8	2.630	25.4 \pm 0.2
980	4.038	0.0026	1.770	9.22	84.1	85.9	3.480	33.5 \pm 0.2
1040	5.678	0.0012	7.084	10.8	92.9	62.4	3.549	34.2 \pm 0.2
1100	7.738	0.0012	10.97	6.32	98.0	57.5	4.460	42.8 \pm 0.4
1200	14.69	0.0320	33.00	0.265	98.2	32.5	4.901	47.0 \pm 8.4
1450	13.05	0.0720	17.70	2.24	100	59.5	7.791	74.2 \pm 1.1
total fusion age = 26.7								
717-120 muscovite (J = 0.005374; wt. = 32.50 mg)								
600	138.3	0.1612	370.4	0.028	0.169	17.7	28.88	260.3 \pm 195
660	25.14	0.0442	78.83	0.266	1.77	6.51	1.808	17.4 \pm 17.6
730	15.87	0.0186	45.48	0.707	6.00	14.2	2.391	23.0 \pm 4.3
790	7.609	0.0067	19.74	2.53	21.2	22.1	1.741	16.8 \pm 1.6
850	2.680	0.0010	2.336	1.60	30.8	62.7	1.954	18.8 \pm 2.1
910	2.599	0.0012	1.440	1.32	38.7	68.4	2.138	20.6 \pm 2.2
970	5.076	0.0032	9.810	1.16	45.7	37.7	2.141	20.6 \pm 4.5
1030	5.330	0.0151	11.18	1.01	51.8	33.1	1.992	19.2 \pm 4.3
1100	4.300	0.0015	6.100	3.87	75.0	54.9	2.462	23.7 \pm 1.2
1450	7.064	0.0068	13.12	4.16	100	43.6	3.151	30.3 \pm 1.1
total fusion age = 23.4								
718-290 muscovite (J = 0.005238; wt. = 79.35 mg)								
650	17.18	0.0508	26.33	2.10	1.82	54.4	9.367	87.9 \pm 0.8
740	3.698	0.0043	2.144	7.61	8.43	81.6	3.029	28.9 \pm 0.3
780	2.812	0.0011	0.7304	14.3	20.8	90.8	2.561	24.4 \pm 0.2
820	2.950	0.0009	0.9738	22.4	40.3	88.9	2.626	25.1 \pm 0.1
870	3.293	0.0007	0.3195	23.1	60.3	95.9	3.162	30.1 \pm 0.1
920	3.431	0.0018	0.3425	11.5	70.2	95.8	3.294	31.4 \pm 0.2
970	3.847	0.0015	0.7517	3.60	73.4	92.6	3.589	34.2 \pm 0.7
1050	3.555	0.0017	0.2320	14.6	86.1	96.9	3.451	32.9 \pm 0.1
1150	3.788	0.0033	0.4147	11.8	96.3	95.6	3.630	34.6 \pm 0.2
1450	4.656	0.0330	1.743	4.22	100	87.8	4.108	39.1 \pm 0.7
total fusion age = 30.8								
718-660 muscovite (J = 0.005304; wt. = 113.91 mg)								
650	18.23	0.5319	12.92	7.17	6.82	79.0	14.42	132.9 \pm 0.5
740	13.42	0.732	1.283	12.1	18.3	96.9	13.01	120.4 \pm 0.4
790	8.572	0.0147	0.7602	14.3	32.0	96.9	8.312	77.8 \pm 0.2
840	7.617	0.0125	0.5081	19.9	50.8	97.5	7.431	69.7 \pm 0.1
870	8.633	0.0153	1.167	13.1	63.3	95.5	8.253	77.3 \pm 0.2
910	10.57	0.0416	0.8590	11.5	74.2	97.2	10.28	95.8 \pm 0.4
980	9.790	0.0430	0.5858	10.4	84.1	97.8	9.584	89.5 \pm 0.2
1050	8.100	0.0354	0.3672	14.6	98.0	98.2	7.958	74.6 \pm 0.2
1120	12.45	0.1352	1.400	1.29	99.2	95.9	12.01	111.4 \pm 2.1
1200	13.23	0.3547	3.868	0.863	100	90.5	12.07	112.0 \pm 1.4
total fusion age = 88.2								

$^{40}\text{Ar}^*$ = radiogenic argon, $^{39}\text{Ar}_K$ = argon produced by nuclear reaction on potassium.

Age spectra with monotonically decreasing ages have been attributed to the incorporation of ^{40}Ar into anion vacancies in the crystals that subsequently are released earlier during the step heating procedure than are the radiogenic ^{40}Ar , which is held in cation sites (Harrison and McDougall, 1981; Zeitler and Fitz Gerald, 1986). This type of behavior is seen in all of the multigrain K-feldspar samples (Fig. 1). Quite often, the contamination of "excess" ^{40}Ar is confined to the first few percent of ^{39}Ar released from a feldspar. Because of the inherent limitation of the laser system (see below), we were unable to limit the temperature of the initial steps to $\sim 550^\circ\text{C}$, the temperature at which most of this contaminating Ar is often driven off. It may be, therefore, that in cases such as

grain 417 (Fig. 5), that in the first step, which makes up 27% of the ^{39}Ar , most of the contaminating ^{40}Ar is in the first 5% of ^{39}Ar released but that it appears to be affecting a greater part of the ^{39}Ar due to the low resolution of the age spectra. This phenomenon of excess ^{40}Ar in the early portions of gas released can be superimposed on an age spectra produced by episodic loss or slow cooling (e.g., grain 459, Fig. 7).

To date, the majority of single-crystal $^{40}\text{Ar}/^{39}\text{Ar}$ dating using lasers has been on volcanic rocks (e.g., Dalrymple and Duffield, 1988; LoBello et al., 1987; Deino, 1989). In these studies it was unnecessary to produce detailed age spectra due to the simple thermal history of the rocks. This study demonstrates that single-crystal $^{40}\text{Ar}/^{39}\text{Ar}$ dating using the laser

ODP Leg 116 multi-grain samples

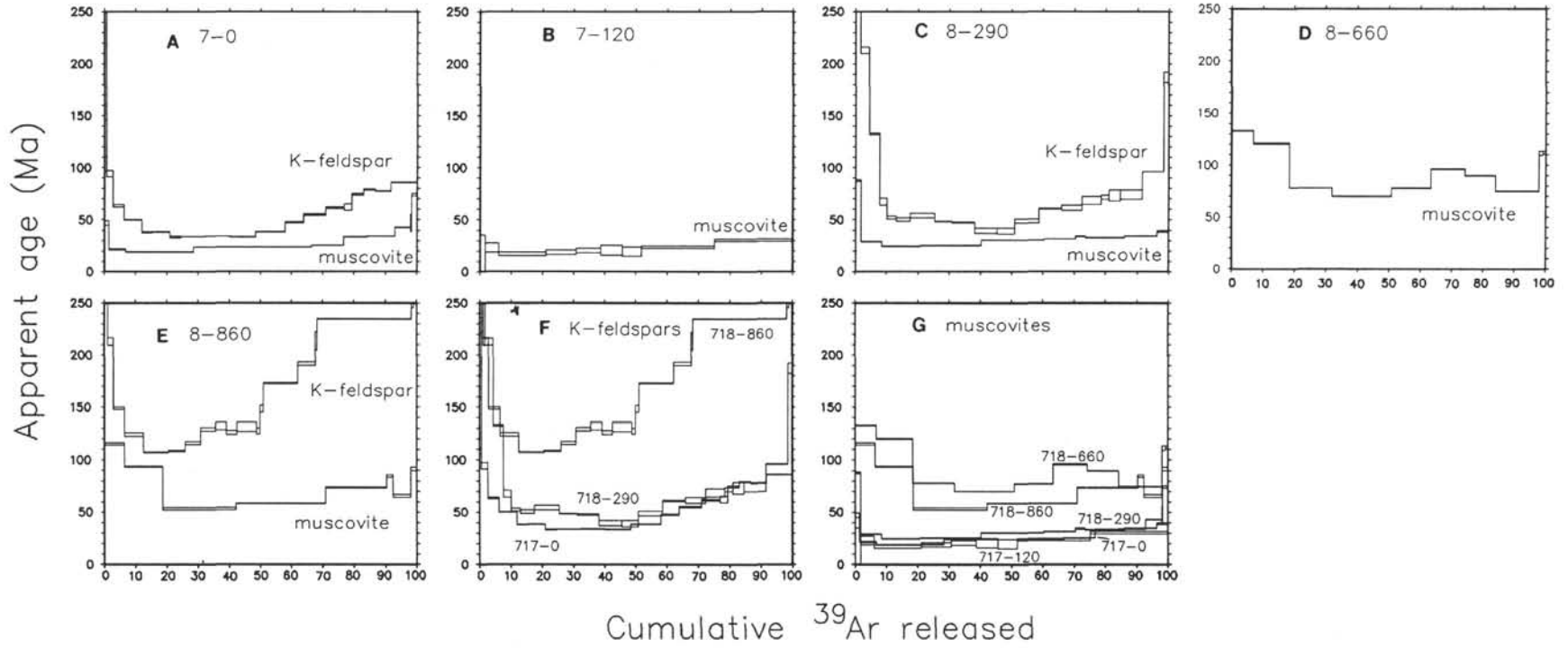


Figure 1. $^{40}\text{Ar}/^{39}\text{Ar}$ age spectra for bulk separates of K-feldspar and muscovite from Sites 717 and 718. **A.** Muscovite and K-feldspar for level 717-0, **B.** Muscovite for level 717-120, **C.** Muscovite and K-feldspar for level 718-290, **D.** Muscovite for level 718-660, **E.** Muscovite and K-feldspar for level 718-860, **F.** Composite of the three K-feldspars, **G.** Composite of the four muscovites.

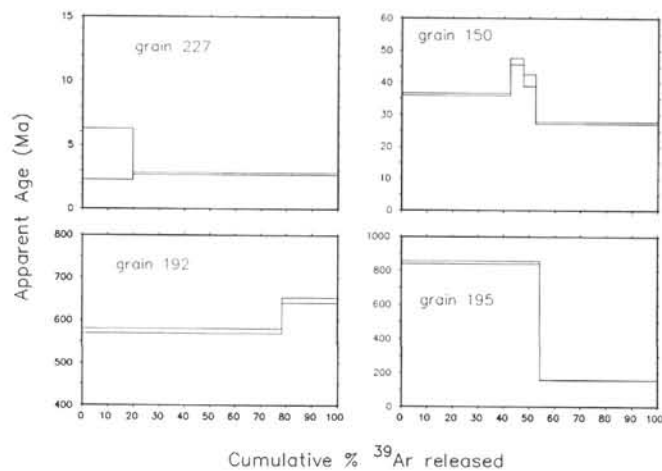


Figure 2. Age spectra diagrams for K-feldspars from level 717-220.

heating method can reveal the same kind of age spectra as in conventional heating of multigrain samples. The variability of these results, both in the age of the grains and the form of the age spectra, also clearly demonstrates the necessity of such a detailed investigation when trying to obtain tectonic information from sedimentary samples.

Figure 10 shows the mineral age for both single and multigrain samples of K-feldspar and muscovite vs. stratigraphic age. Note the curve that represents the 1:1 relationship between the mineral and stratigraphic age. The individual K-feldspars show a very large range in apparent ages in any level, up to 1660 Ma, and in each case have at least one crystal that plots on the 1:1 curve (Fig. 10A). The muscovite data in Figure 10B also show crystals that plot essentially on the 1:1 line but with much smaller age ranges. All but two muscovites plot on or above this line within the uncertainty on the stratigraphic age and the 1σ uncertainty on the mineral age. The two muscovites that fall below this line (grains 710 and 704) have anomalously high $^{36}\text{Ar}/^{39}\text{Ar}$ values that may be due to contamination of mass 36 with hydrocarbons. This may also be the case with other samples but these are the only two for which we have objective criteria indicative of a problem.

We take the closure temperature (T_c) of the muscovites analyzed here to be $\sim 350 \pm 25^\circ\text{C}$ (Purdy and Jäger, 1976; Robbins, 1972). The T_c of K-feldspar has a much greater variability in nature, ranging from greater than 300 to $\sim 150^\circ\text{C}$ (Lovera et al., 1989; Foland, 1974; Harrison and McDougall, 1982). The T_c of K-feldspars can often be calculated from diffusion parameters obtained during a step heating experiment. Unfortunately this is not the case for the K-feldspars in this study, for the following reasons:

1. The single crystals were heated in a maximum of five steps, insufficient to define the Arrhenius parameters for a sample.

2. Even if the single crystals were heated in an appropriate number of steps, accurate temperature monitoring is not possible when heating with an Ar laser; therefore, not all of the Ar was extracted from some of the crystals. The temperature during heating is a function of both laser power and the light coupling characteristics of the crystal. Furthermore, as heating proceeds, internal features that couple the power within the crystals tend to anneal, making the crystal transparent to the laser. Note that Tables 2 and 4 differ from Table 3 in two respects. Table 3 reports the laser power of a heating

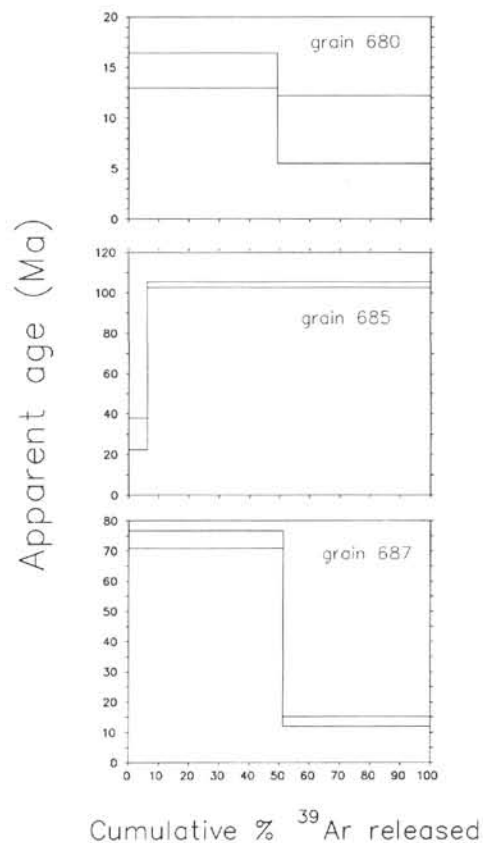


Figure 3. Age spectra diagrams for K-feldspars from level 717-420.

step rather than the temperature and, when more than one step was done on a crystal, reports a "total gas age" rather than a "total fusion age." To test how much Ar was left behind, we took three crystals that apparently did not completely fuse under full laser power (5 W) and heated them in a resistance furnace at 1600°C for 10 min. The gas emitted during this procedure represented approximately 20% of the amount obtained using the laser alone.

3. The bulk separates of K-feldspar heated in the resistance furnace were heated in no less than 19 steps with accurate and precise temperature monitoring. However, the analysis of the individual crystals clearly shows an extreme heterogeneity in the populations of K-feldspars from all levels. Therefore the Arrhenius parameters calculated from these experiments have no meaning, as they result from the mixing of crystals with different diffusion behaviors. We take the T_c of the K-feldspars in this study to be $\sim 200^\circ\text{C}$. We feel this estimate is a reasonable lower bound, as rarely do these values fall below 170°C . In particular, a survey of 51 K-feldspars from plutonic and metamorphic rocks in the eastern Himalayas and southern Tibetan Plateau revealed minimum T_c 's strictly greater than 180°C and usually in the range 250 to 300°C (Copeland, 1990). We therefore take the age minima for the individual K-feldspar crystals analyzed to record the last time at which the crystals were at a temperature of $\sim 200^\circ\text{C}$. In addition to the problems of defining the T_c 's for these crystals discussed above, there may be an additional uncertainty in this estimate. The low resolution of these age spectra (maximum five steps) may mask the true minimum age of the sample; K-feldspars often have a range in ages that correspond to the times at which various parts of the crystal closed

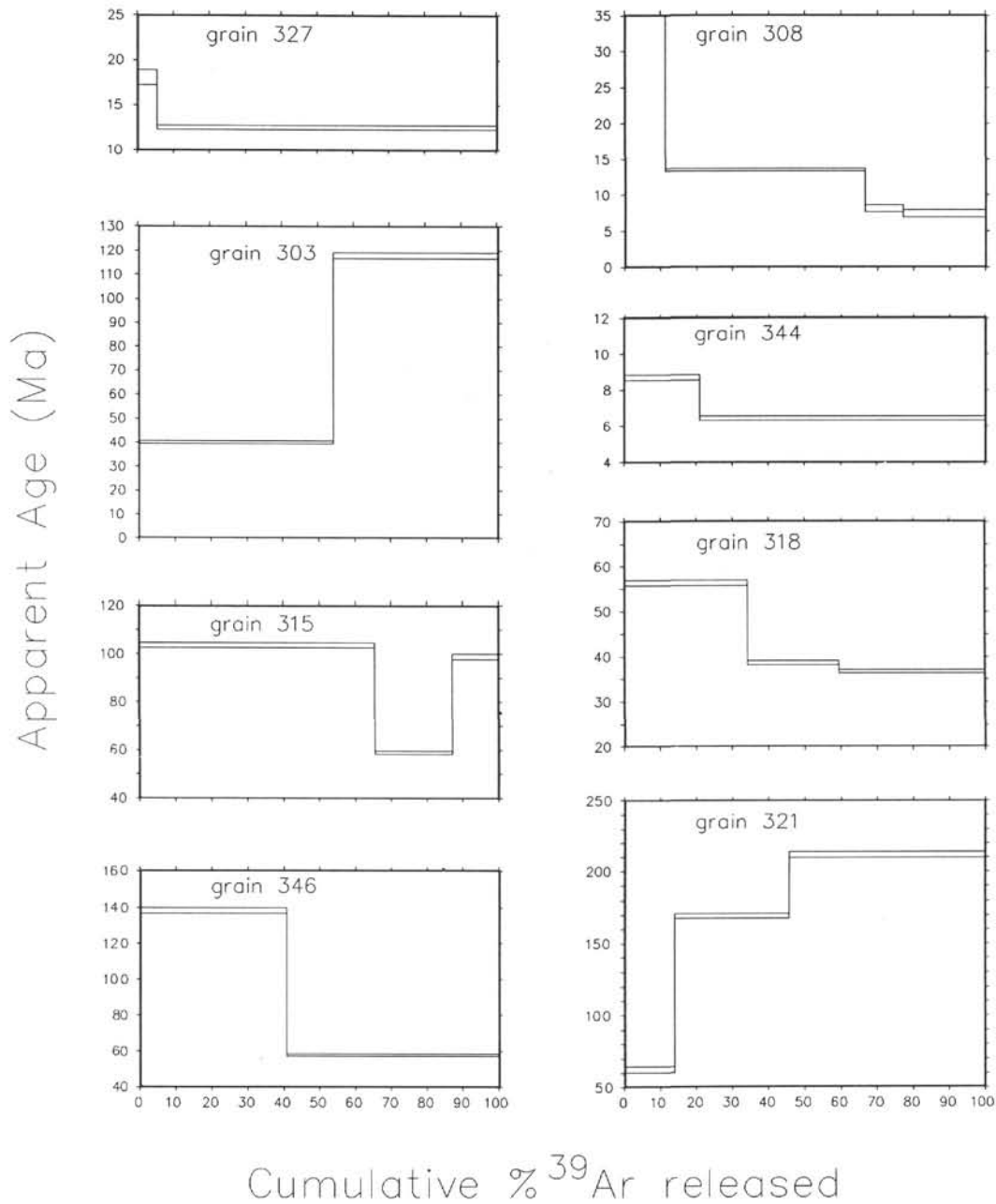


Figure 4. Age spectra diagrams for K-feldspars from level 717-520.

to Ar loss (Lovera et al., 1989). That is, K-feldspars can have more than one T and the relatively small number of steps done on these single crystals may result in the mixing of Ar from different parts of the crystal, which closed at different temperature (and different times). Therefore, for most of our samples (save the ones that plot on the 1:1 line in Fig. 10) we cannot be sure an even younger age could not have been obtained if analysis of more steps were possible. The stars in Figure 10, which represent the weighted average of the single-crystal analyses, and the squares with X's, the total fusion ages of the multigrain separates, give a generally similar trend but differ in detail (see Table 5). The most pronounced difference is seen in the K-feldspars from level 717-220. The total fusion age from the 25.5-mg analyzed is 54.3 Ma, whereas the weighted

average of eight single crystals analyzed is 727 Ma (Table 5). This weighted average is dominated by a single crystal (grain 139), the oldest analyzed and also one of the largest. These results indicate that, whereas analysis of a dozen crystals may be indicative of the range of ages present in any stratigraphic interval, it is unlikely to be representative of the average age in that interval. The same can be said for the muscovites, as the results from the bulk separates are older than the oldest single crystal analyzed in every case except perhaps one (Fig. 10B). This is probably due to the fact that, when selecting single crystals for laser heating, we were biased toward the largest crystals (this was particularly so for the muscovites). The results from the bulk analyses suggest that the smallest crystals are older.

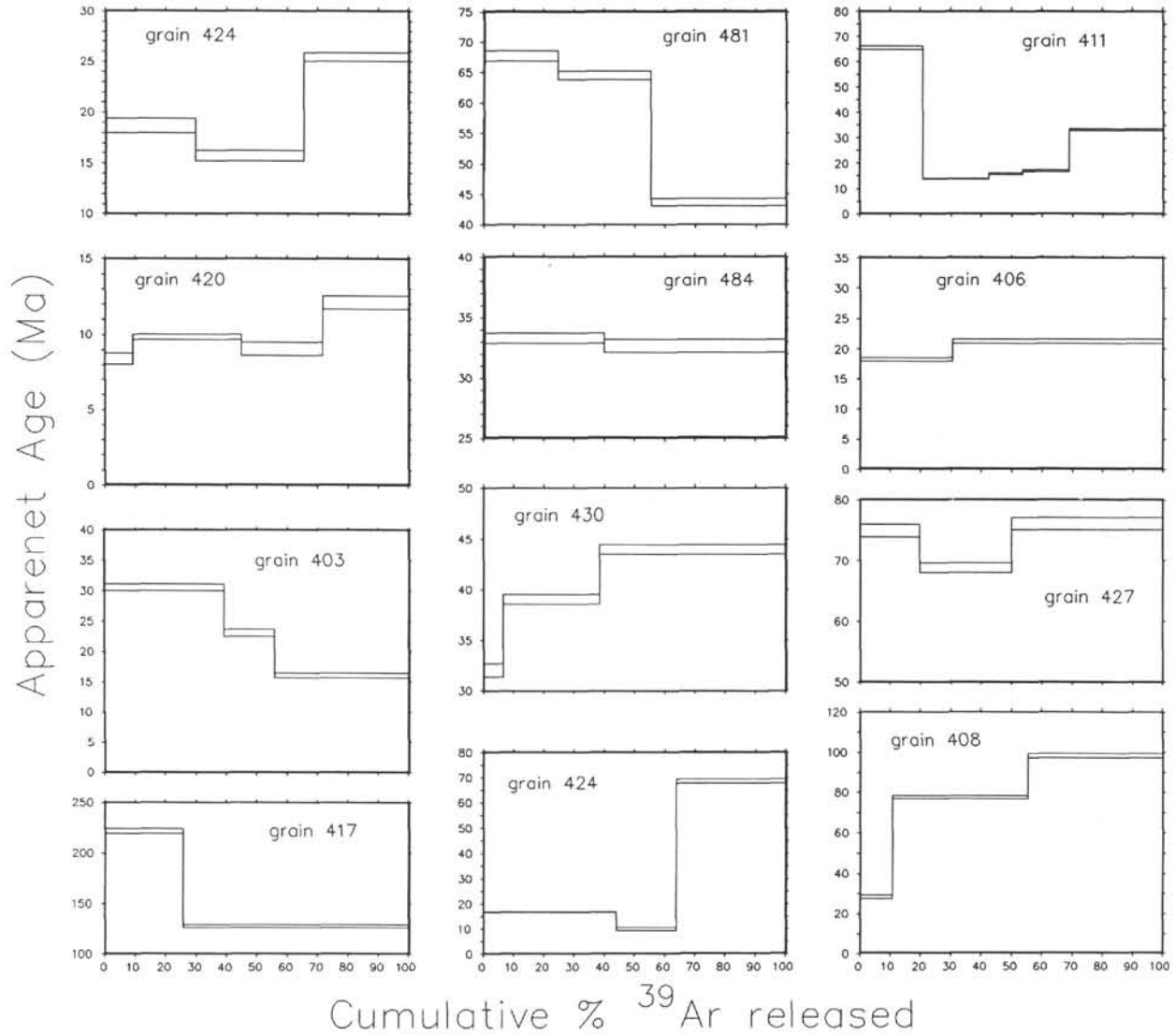


Figure 5. Age spectra diagrams for K-feldspars from level 717-720.

Table 3 shows a wide variation in $^{37}\text{Ar}/^{39}\text{Ar}$ (this value is proportional to the Ca/K in the crystal) for the individual K-feldspars. Most of the single crystals analyzed have $^{37}\text{Ar}/^{39}\text{Ar}$ less than 0.1. With a few exceptions, grains with greater than 3×10^{-15} moles of ^{39}Ar have $^{37}\text{Ar}/^{39}\text{Ar}$ less than 0.03, whereas grains with less ^{39}Ar (smaller grains) have higher $^{37}\text{Ar}/^{39}\text{Ar}$. These facts may indicate that when choosing large grains more potassic feldspars are chosen, whereas the small ones (particularly the very smallest ones in the multigrain samples) may have a plagioclase component. Given that plagioclase is much more susceptible to the uptake of "excess" Ar than K-feldspar (McDougall and Harrison, 1988), this could imply that the older, smaller grains in the bulk contain a greater plagioclase component. However, plagioclase is not revealed in the $^{37}\text{Ar}/^{39}\text{Ar}$ values for the multigrain K-feldspar samples (Table 2). This may be due to the high K concentration in the larger grains overwhelming the low-K, high-Ca concentration of the small grains, or to the inclusion of a major component of (older) K-feldspars as well as a subordinate component of plagioclase feldspar or, most likely, both, in the small grains. All the grains that plot on or near the 1:1 correlation line in Figure 10A have high K/Ca values, with

one notable exception, grain 225, which has an age of 2.4 ± 0.7 Ma.

DISCUSSION

The results shown in Figure 10 indicate that since the early Neogene and continuing to the present there has been a component of essentially zero-age sediment in the southern, and presumably other, parts of the Bengal Fan. It should be emphasized that these minimum ages coincide with the *lowest possible ages* for grains in their given stratigraphic interval and not simply some lower bound that may be exceeded with more sampling. The facts that these zero-age grains were identified after a maximum of thirteen single K-feldspars and 12 muscovites were analyzed from each level suggests that this first-cycle sediment is a statistically significant, and therefore tectonically important, component of the Bengal Fan. These observations provide a stratigraphic link between the Bengal Fan and tectonic events in the source area. Redeposition of older parts of the fan may have influenced the stratigraphic thicknesses of the Bengal Fan, but is likely to have been negligible. Therefore, the significant volume of Miocene sediment in the southern

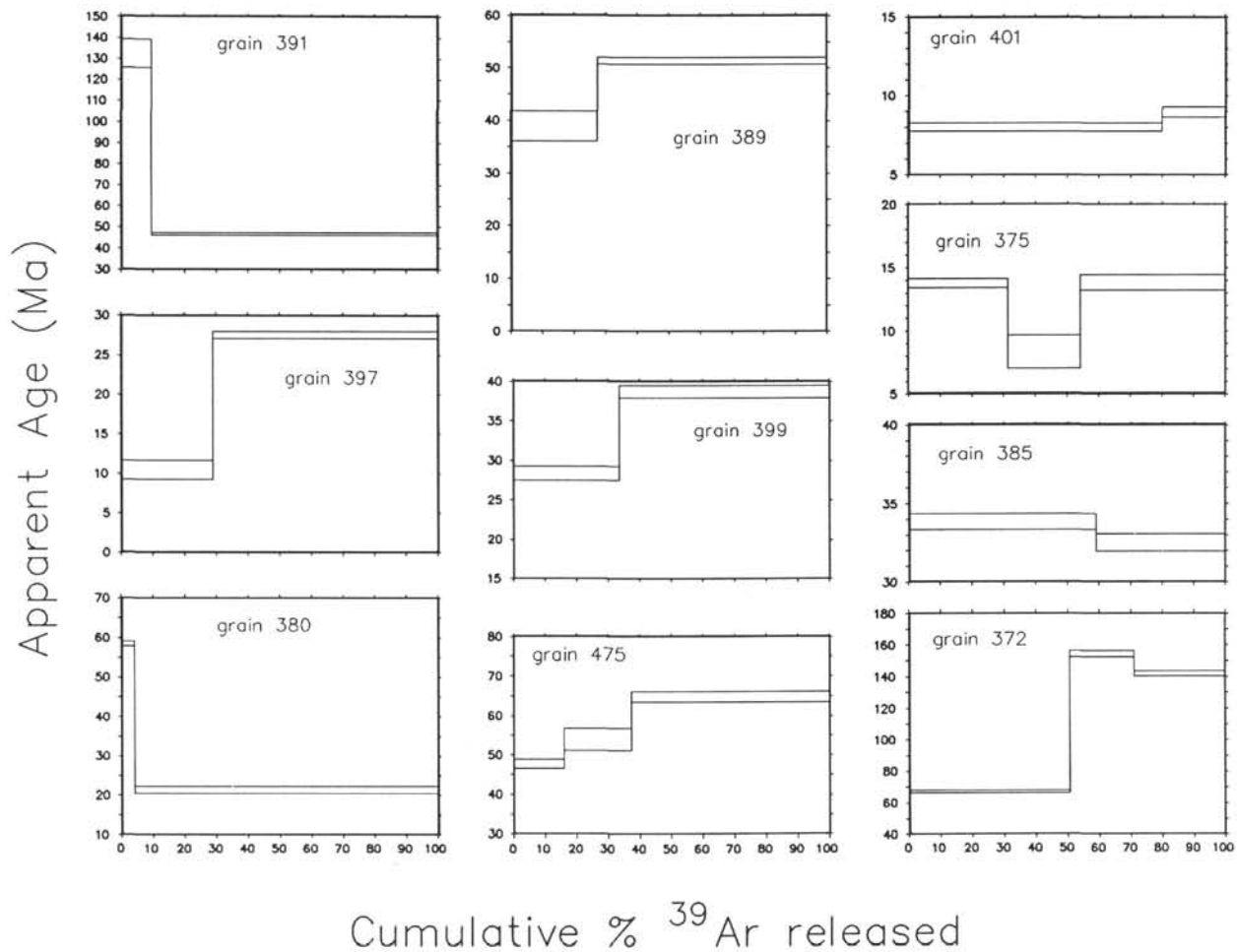


Figure 6. Age spectra diagrams for K-feldspars from level 718-560.

part of the fan must be the result of rapid uplift and erosion in the southern Tibetan Plateau or Himalayas at this time—an inference previously made from land-based studies (Copeland et al., 1987a, b).

Note that both the range and total fusion ages of the K-feldspars from a particular stratigraphic horizon are always larger than those from the muscovites from the same stratigraphic level (Fig. 10, Table 5). Given that the T_c of muscovite is 100° to 200°C greater than the T_c of K-feldspar, this would seem somewhat counterintuitive. We infer that this apparent paradox can be explained if we now draw our attention to the rocks in the source area that probably did not experience rapid uplift immediately prior to transport and deposition in the Bengal Fan. These rocks, which are made up of many rock types, include Triassic sandstone (in the Himalayas) and Proterozoic-Archean gneisses (in the Indian shield), contain much more K-feldspar than muscovite. Just the opposite can be said for the rocks near the main central thrust (MCT) and the main boundary thrust (MBT), exposed on the southern slope of the Himalayas, which are mostly schists. The addition of moderate or even small quantities of sediment derived from these older rocks to sediment derived from the recently rapidly uplifted rocks could greatly bias the average age of the K-feldspar but barely change the average age of the muscovite. Sedimentological data, which suggest a dominant source at the Ganges Delta with a subordinate contribution from the Indian-Sri Lankan margin (Bouquillon et al. and Yokoyama et

al., both this volume; Ingersoll and Suczek, 1979), is consistent with this hypothesis.

Figure 11 shows that subsequent to about 13 Ma the average age of the muscovite and K-feldspar in the southern Bengal Fan maintained constant values of about 30 and 70 Ma, respectively. Prior to this time the average ages of muscovite and K-feldspar were as high as 70 and 183 Ma. These facts suggest that it was not until about 14 to 13 Ma that the younger, schist-rich provenance became dominant.

The fact that the minerals analyzed here record the times they were last at temperatures of at least 200°C (perhaps as much as 280°C) indicates very rapid unroofing and transport rates for the zero-age sediments. We can assume that once a grain reaches the surface it is transported to the basin essentially instantaneously ($\ll 100$ k.y.). Even with this time set to zero, very little time is available for unroofing of these minerals. The erosion rates needed to produce the observed age distribution would significantly perturb isotherms, so it is not possible to calculate a depth from the T_c . However, the minimum depth of mineral closure was probably no less than 5 km. Therefore, erosion rates in excess of 5 mm/yr are indicated. This is a conservative estimate, and much higher rates may have existed over brief intervals. To maintain such rapid erosion rates, significant topographic relief must have existed. Thus these erosion rates were probably accompanied by uplift rates (relative to sea level) that were greater than or equal to 5 mm/yr, thus producing significant topographic relief

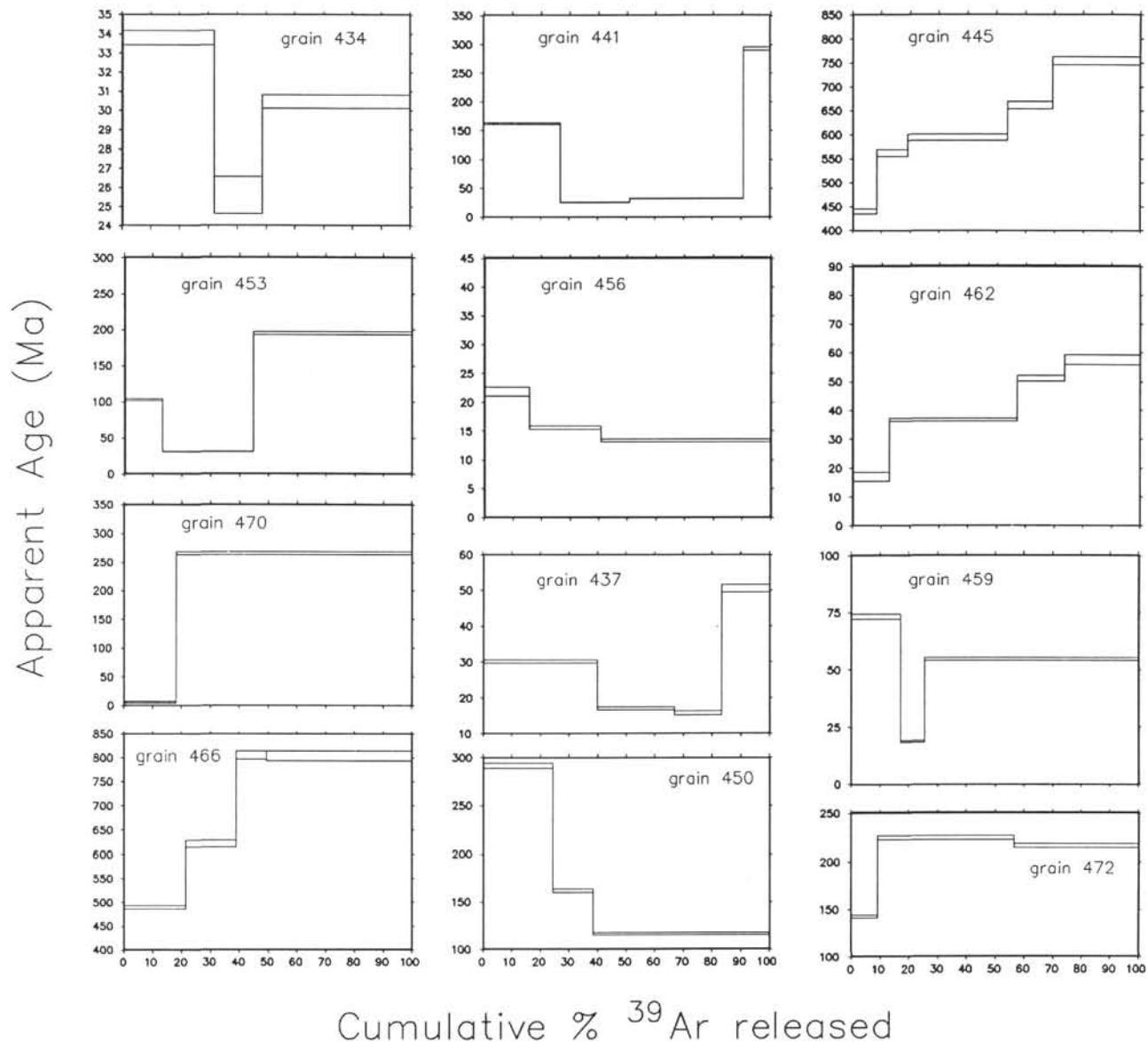


Figure 7. Age spectra diagrams for K-feldspars from level 718-660.

on the southern margin of the Tibetan Plateau by about 18 to 15 Ma. The paucity of granulite facies rocks in the Himalayas and southern Tibetan Plateau (see Le Fort, 1989) indicates that the distribution of ages reported in this study could not be the result of a single locality experiencing rapid uplift and erosion over the last 20 Ma. This uplift must have been distributed throughout the orogen during the entire Neogene with a very rapid pulse of uplift occurring in one location for only a brief time. The apatite fission-track data of Corrigan and Crowley (this volume) may suggest minimum orogen-wide average erosion rates over the last 18 Ma in the range of 0.5 to 1.5 mm/yr. Fission-track ages from detrital zircons in the Siwalik sandstones of northern Pakistan and India (not a part of the drainage basin of the Bengal Fan) also suggest rapid uplift within the Himalayas over the last ~20 Ma (Zeitler et al., 1986). Recently, very young (<5 Ma) hornblende, mica, and K-feldspar $^{40}\text{Ar}/^{39}\text{Ar}$ ages from near the MCT in central Nepal have been interpreted to be the result of resetting by hot fluids passing along the MCT in response to movement on the MBT (Harrison et al., 1989). If this hot fluid flow was a

pervasive feature along the MCT at 6 to 3 Ma, the very steep geotherms associated with this hydrothermal activity would suggest a total amount of unroofing on the order of 4 to 8 km, rather than as much as 13 to 15 km, the depth of the muscovite closure (assuming a 25°C/km geotherm). Therefore, uplift rates experienced by the grains with $^{40}\text{Ar}/^{39}\text{Ar}$ apparent ages essentially equal to the stratigraphic age may have been much lower, say 1 to 3 mm/yr rather than 5 to 10 mm/yr.

Relating our results to uplift rates would be inappropriate if the turbidites of the Bengal Fan contain a significant component of volcanogenic material. For example, the distribution of mineral age vs. stratigraphic age off the coast of Central America may look similar to that shown here for the southern Bengal Fan, but this area has clearly not experienced sustained Tertiary uplift greater than 5 mm/yr. Fortunately, the volcanic origin of the material in the Bengal Fan can be essentially ruled out. No sanidine was observed in the K-feldspar separates, and muscovite is a very rare product of explosive volcanism. The K-feldspar is sub-angular to rounded and commonly frosted on all surfaces. Moreover,

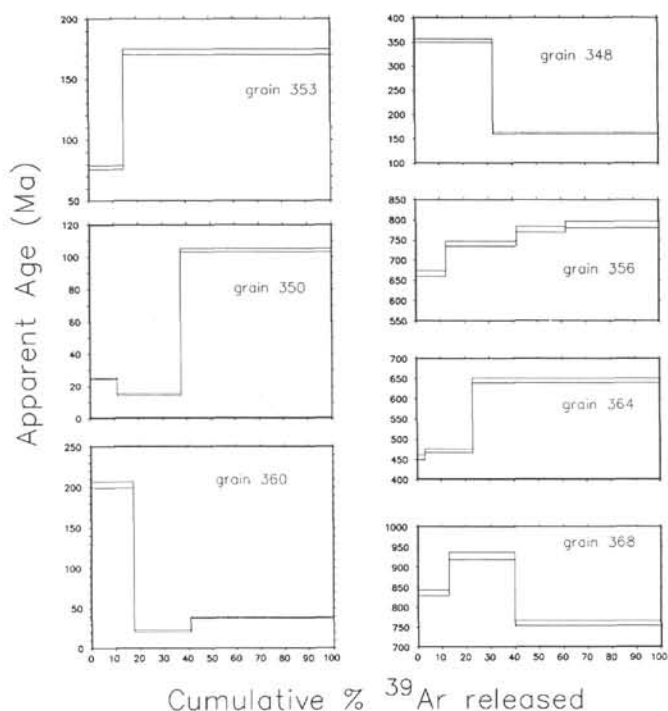


Figure 8. Age spectra diagrams for K-feldspars from level 718-760.

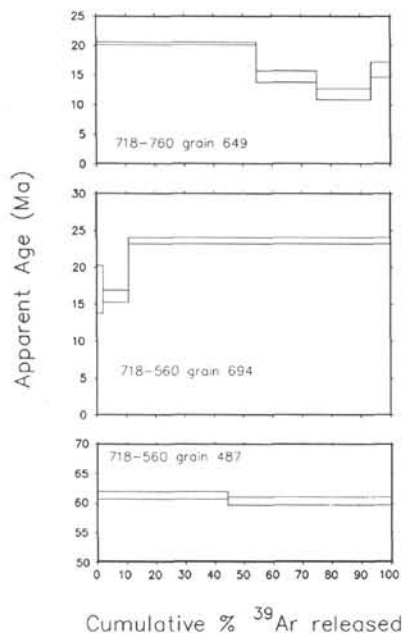


Figure 9. Age spectrum diagrams for muscovites.

very few Neogene volcanoes have been reported from the drainage basin of the Bengal Fan. Some mid-Miocene volcanic rocks have been reported by Coulon et al. (1986) from one locality in the southern Tibetan Plateau, but as far as is known these are not extensive and are therefore unlikely to have contributed significantly to the Bengal Fan. Our observations are consistent with the conclusions of Ingersoll and Suczek (1979), who found the Miocene through Pliocene turbidites of the Bengal Fan at DSDP Site 218 (approximately 1100 km northeast of ODP Site 116) to be essentially composed of sands from gneissic, sedimentary, and metasedimentary ter-

ranes of the Himalayas. In fact, of approximately 6,600 lithic grains counted, only one grain was clearly identifiable as an andesitic fragment. An authigenic origin for any of the K-feldspars can also be ruled out based on both textural evidence and an estimate of the current temperature at the base of holes at Site 718—30° to 38°C; temperatures in shallower portions of the hole are much lower (Cochran, Stow, et al., 1989).

Whereas it is clear that there have been events that have affected the relative contribution of the various source areas of the Bengal Fan over the last 18 Ma (Fig. 11), we infer that the relative ease with which the zero-age grains were identified (as few as four grains analyzed) indicates that a rapidly uplifting and eroding mountain range has been an important component of this provenance during this time. Moreover, given that we can identify this rapid-uplift component, it is notable that grains which do not record such an episode of rapid erosion in their $^{40}\text{Ar}/^{39}\text{Ar}$ systematics may have experienced such an episode nonetheless. For example, a gneiss that was metamorphosed to temperatures greater than 350°C in the Proterozoic and subsequently spent the Phanerozoic at temperatures of 200° to 100°C would have muscovite and K-feldspar that today would give $^{40}\text{Ar}/^{39}\text{Ar}$ ages greater than 600 Ma. If such a sample experienced a brief pulse of rapid uplift and denudation, say from 3 km depth to the surface in less than 1 m.y., such an episode would not be detectable using the techniques in this study. It is certainly the case that for every grain which plots on the 1:1 line in Figure 10, at least 3 km of overburden had to be shed for the 1:1 grains to record the brief pulse of uplift. The vast majority of the grains shed into the Bengal Fan from this overburden will not, however, record the pulse of erosion that they did indeed experience. Therefore, the volume of sediment in the Bengal Fan that experienced rapid uplift and denudation immediately prior to deposition inferred from Figure 10 is a minimum and, quite likely, a serious underestimate.

Although the specific source of an individual grain cannot be ascertained, available data from the source area strongly suggest some possible locations for the material that plots on the 1:1 correlation curve in Figure 10. Results from 25 km southwest of Lhasa (Copeland et al., 1987a) and just north of Mt. Everest (Copeland et al., 1987b) suggest widespread and rapid unroofing in the early Miocene that may be responsible for the older material that plots on the 1:1 line. It cannot be unambiguously stated where the material with zero age at the time of deposition in the intermediate levels (717-720, 718-290, 718-560) came from due to lack of similar cooling ages on land that correspond to these times of deposition. However, for the material with stratigraphic age less than 9 Ma it seems clear that the source of this material was the region immediately north of the MCT (Maluski et al., 1988) or between the MCT and MBT (e.g., Hubbard and Harrison, 1989; Kai, 1981; Maluski et al., 1988). The MCT and MBT are the two structures that have accommodated the most convergence between India and Asia during the Neogene. Estimates of total movement on these structures range from ~200 km and ~100 km for the MCT and MBT, respectively (Molnar, 1984). From available data (Curry and Moore, 1971; Moore et al., 1974; Rabinowitz et al., 1988) we estimate the volume of the post-Eocene material in the Bengal Fan to be 15 and 20 million km³. Such vast quantities of material produced in a relatively short time must have come from an area that experienced significant and frequent tectonic disruptions. The area adjacent to the MCT and the MBT is certainly such an area and the isotopic data presented here suggests that, since at least 9 Ma, this region has been a major source area for the Bengal Fan. The paucity of any observed cooling ages on land in the range

Table 3. $^{40}\text{Ar}/^{39}\text{Ar}$ step heating and total fusion results from single crystals of muscovite and K-feldspar from samples at Sites 717 and 718.

Power (mW)	$^{40}\text{Ar}/^{39}\text{Ar}$	$^{37}\text{Ar}/^{39}\text{Ar}$	$^{36}\text{Ar}/^{39}\text{Ar}$ (E-3)	^{39}Ar (E-15 mol)	% ^{39}Ar released	$^{40}\text{Ar}^*$ %	$^{40}\text{Ar}^*/^{39}\text{Ar}_\text{K}$	Age \pm 1 s.d. (Ma)
717-220 K-feldspar ($J = 0.005329$) grain 137								
5000	1.248	0.0893	2.010	2.43	100	37.2	0.627	6.0 ± 0.2
grain 139								
5000	285.3	0.0169	13.97	8.40	100	98.7	285.6	1669 ± 12.5
grain 148								
5000	5.503	0.0116	0.7260	4.12	100	92.6	5.254	49.8 ± 0.5
grain 150								
370	4.108	0.0058	0.8780	3.10	42.5	86.9	3.813	36.3 ± 0.4
550	2.392	0.0496	5.100	0.366	47.5	99.9	4.911	46.6 ± 1.0
800	3.157	0.559	5.311	0.351	52.4	88.4	4.281	40.7 ± 1.9
5000	3.012	0.0054	0.3412	3.47	100	89.4	2.875	27.4 ± 0.3
total gas age = 32.8								
grain 192								
100	71.29	0.0140	2.928	2.71	78.3	98.3	70.39	574.7 ± 5.1
5000	83.06	0.0344	7.247	0.750	100	96.3	80.88	646.6 ± 6.2
total gas age = 590.2								
grain 195								
250	121.7	0.7261	31.22	0.465	54.1	91.7	112.6	847.7 ± 7.9
5000	22.99	0.5184	19.40	0.394	100	72.1	17.26	158.7 ± 1.9
total gas age = 531.8								
grain 225								
5000	2.795	1.592	8.842	0.214	100	5.22	0.2453	2.4 ± 3.7
grain 227								
150	1.961	0.0972	5.024	0.718	19.7	17.7	0.4467	4.3 ± 2.0
5000	0.623	0.0185	1.016	2.92	100	41.1	0.2879	2.8 ± 0.1
total gas age = 3.1								
717-420 K-feldspar ($J = 0.005401$) grain 680								
800	3.396	0.2068	6.318	0.562	49.2	41.9	1.506	14.7 ± 1.7
5000	2.531	0.2795	5.432	0.580	100	33.0	0.9079	8.9 ± 3.4
total gas age = 11.7								
grain 685								
50	7.778	1.063	15.93	0.164	6.21	36.7	3.105	30.1 ± 7.7
5000	11.58	0.0298	2.033	2.48	100	93.7	10.94	104.1 ± 1.4
total gas age = 99.5								
grain 687								
1000	11.45	0.2638	12.67	0.503	51.2	65.8	7.687	73.7 ± 2.9
5000	4.474	0.2715	10.36	0.480	100	28.9	1.392	13.6 ± 1.6
total gas age = 44.4								
grain 690								
5000	1.431	0.0387	2.979	1.01	100	33.2	0.5165	5.1 ± 0.5
717-520 K-feldspar ($J = 0.005351$) grain 302								
5000	15.49	0.0065	3.941	6.30	100	91.9	14.29	132.4 ± 1.4
grain 303								
1000	5.532	0.0089	4.329	3.34	54.0	75.1	4.217	40.1 ± 0.6
5000	13.57	0.0053	2.952	2.84	100	92.1	12.66	117.8 ± 1.3
total gas age = 75.8								
grain 308								
80	221.5	0.0870	19.80	0.544	11.3	96.6	215.6	1380 ± 16.1
350	1.686	0.0084	0.8050	2.67	66.6	64.6	1.413	13.5 ± 0.2
800	1.451	0.0945	1.947	0.506	77.1	27.0	0.8459	8.1 ± 0.5
5000	1.760	0.0332	3.238	1.11	1000	31.1	0.7685	7.4 ± 0.5
total gas age = 165.5								
grain 310								
5000	7.028	0.0320	9.709	1.05	100	55.5	4.125	39.2 ± 1.0
grain 315								
200	11.49	0.0128	1.282	4.19	65.5	95.6	11.08	103.5 ± 1.0

Table 3 (continued).

Power (mW)	$^{40}\text{Ar}/^{39}\text{Ar}$	$^{37}\text{Ar}/^{39}\text{Ar}$	$^{36}\text{Ar}/^{39}\text{Ar}$ (E-3)	^{39}Ar (E-15 mol)	% ^{39}Ar released	$^{40}\text{Ar}^*$ %	$^{40}\text{Ar}^*/^{39}\text{Ar}_K$	Age \pm 1 s.d. (Ma)
900	7.446	0.0321	4.053	1.38	87.0	79.2	6.215	58.8 \pm 0.6
5000	12.24	0.0421	5.499	0.829	100	80.2	10.58	99.0 \pm 1.1
								total gas age = 93.3
grain 318								
400	6.685	0.0175	2.380	2.73	34.3	85.5	5.947	56.3 \pm 0.6
1100	4.712	0.0200	2.077	2.00	59.5	80.5	40.64	38.7 \pm 0.4
5000	4.396	0.0049	1.680	3.23	100	84.2	3.860	36.7 \pm 0.4
								total gas age = 43.9
grain 321								
250	7.976	0.0441	4.600	0.478	13.9	74.2	6.584	62.2 \pm 2.1
1000	19.67	0.0194	3.984	1.09	45.7	89.8	18.46	169.3 \pm 1.8
5000	25.20	0.0223	6.150	1.86	100	91.6	23.35	211.6 \pm 2.1
								total gas age = 177.4
grain 326								
5000	7.045	0.0018	1.464	5.91	100	92.1	6.576	62.1 \pm 0.6
grain 327								
1000	1.381	0.1180	0.0000	0.303	5.57	68.3	1.886	18.0 \pm 0.8
5000	1.649	0.0080	1.046	5.13	100	73.3	1.305	12.5 \pm 0.2
								total gas age = 12.8
717-520 K-feldspar grain 340								
1000	3.380	0.1218	5.435	0.775	25.5	41.0	1.746	16.7 \pm 1.4
5000	8.853	0.0781	3.341	2.26	100	84.7	7.835	73.8 \pm 0.8
								total gas age = 59.2
grain 343								
5000	62.26	0.7104	31.06	0.239	100	83.3	53.11	449.6 \pm 5.6
grain 344								
500	1.609	0.0699	2.274	0.635	21.1	37.2	0.9052	8.7 \pm 0.2
5000	1.324	0.1097	2.115	2.38	100	45.6	0.6703	6.4 \pm 0.1
								total gas age = 6.9
grain 346								
500	16.25	0.0240	4.246	1.34	40.8	90.6	14.96	138.4 \pm 1.5
5000	6.965	0.0234	2.771	1.95	100	85.0	6.112	57.8 \pm 0.6
								total gas age = 90.7
717-720 K-feldspar (J = 0.005354) grain 403								
650	3.861	0.0150	2.109	2.75	39.3	79.5	3.203	30.6 \pm 0.5
1900	3.397	0.0202	3.201	1.15	55.8	63.1	2.416	23.1 \pm 0.6
5000	2.094	0.0122	1.283	3.09	100	73.7	1.679	16.1 \pm 0.4
								total gas age = 23.0
grain 406								
700	2.446	0.0365	1.733	1.52	30.5	67.3	1.900	18.2 \pm 0.3
5000	2.760	0.0210	1.706	3.46	100	76.5	2.221	21.3 \pm 0.3
								total gas age = 20.4
grain 408								
100	5.101	0.0839	7.072	0.706	10.7	50.9	2.980	28.4 \pm 0.9
1000	9.307	0.0131	3.567	2.94	55.3	86.7	8.218	77.3 \pm 0.8
5000	11.56	0.0038	3.536	2.95	100	89.3	10.48	98.0 \pm 1.0
								total gas age = 81.3
grain 411								
150	7.496	0.0118	1.814	3.75	20.7	90.7	6.924	65.5 \pm 0.7
600	1.946	0.0058	1.525	3.94	42.5	70.4	1.460	14.0 \pm 0.2
1000	2.217	0.0100	1.750	2.01	53.6	67.6	1.665	16.0 \pm 0.3
1600	2.384	0.0129	1.907	2.78	69.0	69.4	1.786	17.1 \pm 0.4
5000	4.144	0.0097	2.131	5.62	100	81.9	3.479	33.2 \pm 0.4
								total gas age = 31.4
grain 417								
900	26.54	0.0249	6.181	1.67	26.8	91.8	24.67	223.4 \pm 2.5
5000	14.52	0.0084	3.145	4.55	100	92.6	13.55	126.1 \pm 1.3
								total gas age = 152.2
grain 420								
120	1.764	0.0333	2.891	0.845	9.19	37.0	0.8762	8.4 \pm 0.4

Table 3 (continued).

Power (mW)	$^{40}\text{Ar}/^{39}\text{Ar}$	$^{37}\text{Ar}/^{39}\text{Ar}$	$^{36}\text{Ar}/^{39}\text{Ar}$ (E-3)	^{39}Ar (E-15 mol)	% ^{39}Ar released	$^{40}\text{Ar}^*$ %	$^{40}\text{Ar}^*/^{39}\text{Ar}_K$	Age \pm 1 s.d. (Ma)
300	1.662	0.0105	2.036	3.30	45.0	57.8	1.025	9.9 \pm 0.2
1200	1.789	0.0016	2.746	2.46	71.8	48.2	0.9418	9.1 \pm 0.4
5000	2.303	0.0083	3.402	2.60	100	50.5	1.262	12.1 \pm 0.4
total gas age = 10.1								
grain 424								
750	2.249	0.0112	1.536	3.36	44.1	72.6	1.760	16.9 \pm 0.2
1500	1.763	0.0206	2.335	1.50	63.8	49.9	1.039	10.0 \pm 0.5
5000	8.263	0.0183	3.275	2.76	100	85.9	7.261	68.7 \pm 0.8
total gas age = 34.3								
717-720 K-feldspar grain 427								
130	9.270	0.0304	4.383	1.37	19.7	82.8	7.941	75.0 \pm 1.0
450	7.876	0.0187	1.899	2.11	50.1	90.0	7.280	68.8 \pm 0.8
5000	8.662	0.0186	1.917	3.47	100	91.8	8.060	76.1 \pm 1.0
total gas age = 73.7								
grain 430								
225	4.644	0.0620	4.261	0.742	6.66	63.8	3.353	32.0 \pm 0.6
600	4.576	0.0097	1.502	3.54	38.4	86.9	4.097	39.1 \pm 0.5
5000	4.983	0.0058	1.110	6.86	100	91.5	4.620	44.0 \pm 0.5
total gas age = 41.6								
grain 478								
400	2.859	0.0241	1.891	2.45	29.7	73.8	2.266	21.7 \pm 0.7
1000	2.392	0.0157	1.355	2.95	65.4	76.5	1.957	18.8 \pm 0.5
5000	3.370	0.0161	1.215	2.86	100	83.5	2.976	28.5 \pm 0.4
total gas age = 23.0								
grain 481								
140	8.020	0.0243	2.769	2.11	24.7	86.7	7.167	67.8 \pm 0.9
400	7.351	0.0145	1.695	2.62	55.4	89.2	6.815	64.5 \pm 0.7
5000	4.995	0.0060	1.240	3.81	100	89.5	4.593	43.7 \pm 0.6
total gas age = 56.1								
grain 485								
250	4.156	0.0689	2.150	1.85	40.1	76.0	3.489	33.3 \pm 0.4
5000	3.968	0.0505	1.741	2.77	100	82.8	3.420	32.7 \pm 0.5
total gas age = 32.9								
718-560 K-feldspar (J = 0.005329) grain 372								
250	8.394	0.0337	4.209	2.36	50.6	83.2	7.116	67.2 \pm 0.8
800	19.07	0.0249	7.742	0.957	71.1	86.2	16.75	154.3 \pm 2.0
5000	17.15	0.0196	5.979	1.35	100	87.5	15.35	141.9 \pm 1.7
total gas age = 106.6								
grain 375								
150	2.417	0.0070	3.178	1.43	31.4	54.2	1.442	13.8 \pm 0.4
600	1.654	0.0303	2.527	1.03	54.1	41.6	0.8734	8.4 \pm 1.3
5000	2.214	0.0259	2.478	2.09	100	61.8	1.448	13.9 \pm 0.6
total gas age = 12.6								
grain 380								
130	3.935	0.4828	16.89	0.122	4.17	89.3	6.183	58.5 \pm 0.7
5000	4.058	0.0151	6.053	2.81	100	52.7	2.234	21.4 \pm 0.8
total gas age = 22.9								
grain 384								
5000	1.576	0.0245	1.760	1.71	100	50.4	1.022	9.8 \pm 0.3
grain 385								
150	4.275	0.0197	2.317	2.72	59.1	81.4	3.555	33.9 \pm 0.5
5000	4.199	0.0212	2.535	1.88	100	77.1	3.415	32.5 \pm 0.6
total gas age = 33.3								
grain 387								
120	8.064	0.0325	3.621	1.77	59.4	84.2	6.960	65.7 \pm 1.2
5000	5.254	0.0706	0.4328	1.20	100	94.3	5.872	55.6 \pm 4.1
total gas age = 61.6								
grain 389								
90	6.993	0.1030	9.718	0.596	27.3	51.7	4.092	38.9 \pm 2.8
5000	7.337	0.0188	6.351	1.59	100	71.1	5.426	51.4 \pm 0.7
total gas age = 48.0								

Table 3 (continued).

Power (mW)	$^{40}\text{Ar}/^{39}\text{Ar}$	$^{37}\text{Ar}/^{39}\text{Ar}$	$^{36}\text{Ar}/^{39}\text{Ar}$ (E-3)	^{39}Ar (E-15 mol)	% ^{39}Ar released	$^{40}\text{Ar}^*$ %	$^{40}\text{Ar}^*/^{39}\text{Ar}_K$	Age \pm 1 s.d. (Ma)
grain 391								
90	18.76	0.1423	14.98	0.358	9.61	72.3	14.31	132.5 \pm 6.8
5000	5.434	0.0084	1.615	3.37	100	87.9	4.921	46.7 \pm 0.5
								total gas age = 55.0
718-560 K-feldspar grain 397								
300	3.063	0.0729	6.570	0.781	28.9	29.1	1.090	10.4 \pm 1.2
5000	3.605	0.0202	2.303	1.92	100	74.8	2.889	27.6 \pm 0.4
								total gas age = 22.6
grain 399								
120	4.860	0.1119	6.470	0.461	33.4	49.1	2.919	27.8 \pm 0.9
5000	5.039	0.0151	3.340	0.918	100	73.1	4.017	38.2 \pm 0.8
								total gas age = 34.7
grain 401								
500	1.598	0.0415	2.461	2.13	80.0	47.6	0.8371	8.0 \pm 0.3
5000	1.629	0.1277	2.257	0.534	100	33.6	0.9339	9.0 \pm 0.3
								total gas age = 8.2
grain 475								
150	8.385	0.1346	11.29	0.454	16.0	54.4	5.020	47.8 \pm 1.2
360	7.875	0.1401	7.308	0.605	37.3	65.5	5.689	54.0 \pm 2.8
5000	8.018	0.0344	3.858	1.78	100	82.7	6.844	64.8 \pm 1.3
								total gas age = 59.8
718-660 K-feldspar ($J = 0.005305$) grain 434								
130	4.368	0.0604	2.694	2.90	32.0	75.6	3.540	33.8 \pm 0.4
400	3.516	0.0901	2.751	1.51	48.6	71.1	2.673	25.6 \pm 1.0
5000	3.653	0.0414	1.474	4.65	100	84.6	3.184	30.4 \pm 0.4
								total gas age = 30.7
grain 437								
110	3.668	0.0077	1.589	3.42	39.9	82.8	3.163	30.2 \pm 0.4
250	2.454	0.0142	2.147	2.31	66.9	68.3	1.784	17.1 \pm 0.5
500	2.682	0.0427	3.376	1.41	83.4	54.8	1.651	15.8 \pm 0.5
5000	6.531	0.0155	3.950	1.43	100	78.4	5.328	50.6 \pm 1.1
								total gas age = 27.7
grain 441								
350	19.02	0.0127	4.566	2.06	27.1	91.5	17.64	162.5 \pm 1.7
950	3.598	0.0399	2.778	1.84	51.3	71.6	2.743	26.3 \pm 0.5
2000	3.872	0.0211	1.297	3.02	90.9	85.4	3.454	33.0 \pm 0.5
5000	35.69	0.0378	9.025	0.695	100	90.7	32.99	292.9 \pm 3.3
								total gas age = 90.1
grain 445								
65	65.70	0.0488	4.348	0.978	8.36	97.2	64.39	533.4 \pm 4.9
150	80.14	0.0191	3.803	1.25	19.0	98.2	78.98	635.2 \pm 5.8
300	83.96	0.0024	3.193	4.05	53.7	98.7	82.98	662.1 \pm 5.7
600	92.51	0.0044	3.365	1.82	69.3	98.6	91.48	718.0 \pm 6.2
5000	104.7	0.0012	3.115	3.59	100	99.0	103.7	795.4 \pm 6.9
								total gas age = 698.1
grain 450								
400	33.76	0.0313	2.989	2.24	24.4	96.8	32.84	291.7 \pm 2.8
900	18.96	0.0229	4.732	1.29	38.5	91.1	17.53	161.5 \pm 1.8
5000	13.03	0.0080	1.647	5.64	100	95.4	12.50	116. \pm 1.2
								total gas age = 165.7
grain 453								
150	12.29	0.0224	4.225	1.65	13.4	87.9	11.0	103.1 \pm 1.3
600	3.713	0.0145	1.532	3.88	44.8	84.8	3.225	30.8 \pm 0.4
5000	22.68	0.0057	4.254	6.81	100	94.0	21.39	195.2 \pm 1.9
								total gas age = 131.2
grain 456								
600	3.699	0.0226	4.673	1.28	15.9	55.6	2.283	21.9 \pm 0.8
1500	2.027	0.0284	1.228	2.01	40.8	71.8	1.629	15.6 \pm 0.3
5000	1.799	0.0079	1.239	4.78	100	73.8	1.397	13.4 \pm 0.2
								total gas age = 15.3

Table 3 (continued).

Power (mW)	$^{40}\text{Ar}/^{39}\text{Ar}$	$^{37}\text{Ar}/^{39}\text{Ar}$	$^{36}\text{Ar}/^{39}\text{Ar}$ (E-3)	^{39}Ar (E-15 mol)	% ^{39}Ar released	$^{40}\text{Ar}^*$ %	$^{40}\text{Ar}^*/^{39}\text{Ar}_K$	Age ± 1 s.d. (Ma)
718-660 K-feldspar grain 459								
90	9.007	0.0217	4.083	1.47	17.2	83.3	7.766	73.3 \pm 1.1
175	3.214	0.0732	4.127	0.714	25.6	50.4	1.963	18.8 \pm 0.3
5000	6.052	0.0064	0.8679	6.37	100	94.2	5.760	54.7 \pm 0.6
								total gas age = 54.9
grain 465								
70	3.789	0.0780	6.697	0.598	12.7	40.2	1.779	17.1 \pm 1.6
170	4.782	0.0304	3.049	2.09	57.2	77.0	3.847	36.7 \pm 0.5
350	7.185	0.0623	5.991	0.777	73.7	69.3	5.383	51.2 \pm 1.0
5000	7.899	0.0574	6.116	1.24	100	73.1	6.060	57.5 \pm 1.7
								total gas age = 42.1
grain 466								
170	58.85	0.0084	1.408	3.20	21.5	99.0	58.40	490.0 \pm 4.5
250	86.97	0.0219	1.957	2.59	39.0	99.1	86.36	684.5 \pm 5.9
1000	112.1	0.0099	4.265	1.55	49.4	98.6	110.8	838.8 \pm 7.0
5000	112.0	0.0058	4.862	7.51	100	98.6	110.5	837.2 \pm 8.2
								total gas age = 735.9
grain 470								
800	2.384	0.0820	5.830	0.534	18.1	19.5	0.6301	6.1 \pm 2.7
5000	31.16	0.0092	4.604	2.42	100	95.1	29.76	226.2 \pm 2.6
								total gas age = 219.1
grain 472								
175	16.54	0.0524	3.872	0.752	9.28	90.1	15.37	142.4 \pm 1.5
350	25.28	0.0108	1.413	3.83	56.4	97.5	24.83	224.7 \pm 2.2
5000	24.35	0.0148	1.592	3.52	100	97.4	23.84	216.3 \pm 2.1
								total gas age = 213.4
718-760 K-feldspar (J = 0.005384) grain 348								
350	42.21	0.0370	6.860	1.32	32.3	94.6	40.15	353.1 \pm 3.4
5000	18.43	0.0145	3.302	2.77	100	93.7	17.42	161.7 \pm 1.6
								total gas age = 223.5
grain 350								
500	4.606	0.0620	6.812	0.842	11.3	50.0	2.561	24.7 \pm 0.4
1000	6.271	0.0224	15.89	1.96	37.7	23.7	1.540	14.9 \pm 0.6
5000	11.55	0.0084	1.615	4.63	100	94.4	11.04	104.1 \pm 1.0
								total gas age = 71.6
grain 353								
1000	14.10	0.0728	20.10	0.441	14.5	53.9	8.128	77.3 \pm 1.6
5000	19.55	0.0144	2.945	2.60	100	94.2	18.65	172.6 \pm 2.4
								total gas age = 158.8
grain 355								
500	5.214	0.0406	6.136	1.19	100	60.3	3.367	32.4 \pm 0.4
grain 356								
100	86.79	0.0941	12.90	0.469	12.5	94.9	82.95	666.1 \pm 6.9
250	96.20	0.0464	6.404	1.10	41.6	97.5	94.27	740.6 \pm 6.2
1000	102.6	0.0564	8.910	0.759	61.8	96.9	99.93	776.7 \pm 6.8
5000	103.5	0.0345	5.790	1.43	100	98.0	101.7	788.0 \pm 7.7
								total gas age = 756.7
grain 360								
500	25.32	0.1020	10.80	0.328	17.6	80.1	22.10	202.8 \pm 3.7
1000	3.605	0.0980	4.390	0.437	41.0	43.8	2.278	22.0 \pm 1.1
5000	4.995	0.0149	3.362	1.10	100	73.0	3.966	38.1 \pm 0.6
								total gas age = 63.3
grain 364								
500	58.76	0.3006	18.63	0.173	3.20	86.2	53.25	454.8 \pm 5.9
1000	56.90	0.0354	4.765	1.08	23.1	97.0	55.46	471.4 \pm 4.4
5000	80.67	0.0091	2.843	4.17	100	98.7	79.80	644.8 \pm 5.6
								total gas age = 604.2
grain 368								
1000	114.8	0.0648	17.73	0.322	13.0	94.3	109.5	836.4 \pm 7.3
1350	127.8	0.0581	9.195	0.673	40.0	97.3	125.0	928.5 \pm 8.6
5000	98.60	0.0224	4.422	1.49	100	98.3	97.26	759.7 \pm 6.3
								total gas age = 815.3

Table 3 (continued).

Power (mW)	$^{40}\text{Ar}/^{39}\text{Ar}$	$^{37}\text{Ar}/^{39}\text{Ar}$	$^{36}\text{Ar}/^{39}\text{Ar}$ (E-3)	^{39}Ar (E-15 mol)	% ^{39}Ar released	$^{40}\text{Ar}^*$ %	$^{40}\text{Ar}^*/^{39}\text{Ar}_K$	Age \pm 1 s.d. (Ma)
717-220 muscovite (J = 0.005354) grain 500								
5000	1.471	0.0114	0.8114	5.12	100	76.0	1.196	11.5 \pm 0.2
grain 502								
5000	3.204	0.1071	8.103	0.440	100	17.2	0.7802	7.5 \pm 0.4
grain 504								
5000	1.302	0.0209	3.206	1.17	100	18.3	0.3197	3.1 \pm 1.0
grain 505								
5000	2.170	0.0169	2.680	2.31	100	55.7	1.343	12.9 \pm 0.5
grain 666								
5000	1.234	0.0089	0.5360	12.7	100	82.3	1.040	10.2 \pm 0.1
grain 667								
5000	4.006	0.0403	7.482	1.99	100	42.8	1.768	17.2 \pm 0.9
grain 668								
5000	1.397	0.0147	1.870	3.61	100	55.0	0.8093	7.9 \pm 0.2
grain 669								
5000	1.728	0.0231	1.612	3.52	100	67.4	1.217	11.9 \pm 0.3
grain 670								
5000	1.616	0.0164	1.751	4.74	100	63.3	1.063	10.4 \pm 0.4
717-420 muscovite (J = 0.005329) grain 678								
5000	2.587	0.0394	4.066	2.05	100	50.7	1.352	13.2 \pm 0.4
717-520 muscovite (J = 0.005222) grain 495								
5000	1.326	0.0041	0.5113	12.0	100	83.5	1.139	11.0 \pm 0.2
grain 496								
5000	2.896	0.0174	5.326	2.74	100	41.7	1.287	12.4 \pm 0.6
grain 497								
5000	3.688	0.0044	1.676	9.64	100	84.4	3.157	30.2 \pm 0.3
grain 498								
5000	1.657	0.0141	2.611	2.02	100	43.2	0.8505	8.2 \pm 0.2
grain 706								
5000	1.962	0.0505	4.220	1.81	100	33.3	0.6826	6.4 \pm 1.4
grain 707								
5000	1.927	0.1050	2.860	1.01	100	52.4	1.052	9.9 \pm 1.6
grain 709								
5000	2.108	0.0153	1.224	4.46	100	79.8	1.711	16.1 \pm 0.5
grain 710								
5000	1.539	0.0312	3.709	2.81	100	25.5	0.4087	3.9 \pm 0.4
717-720 muscovite (J = 0.005313) grain 486								
5000	2.609	0.0069	0.7483	6.24	100	86.3	2.352	22.5 \pm 0.3
grain 698								
5000	1.998	0.0026	1.699	4.55	100	71.6	1.460	13.7 \pm 0.2
grain 700								
500	2.050	0.0206	4.065	2.20	100	38.0	0.8146	7.7 \pm 0.4
grain 701								
500	1.931	0.0184	2.023	3.52	100	54.6	1.298	12.2 \pm 0.4
grain 702								
5000	2.869	0.0469	6.086	1.35	100	32.1	1.038	9.8 \pm 0.8
grain 703								
5000	4.832	0.0335	4.640	2.57	100	70.3	3.427	32.1 \pm 0.5

Table 3 (continued).

Power (mW)	$^{40}\text{Ar}/^{39}\text{Ar}$	$^{37}\text{Ar}/^{39}\text{Ar}$	$^{36}\text{Ar}/^{39}\text{Ar}$ (E-3)	^{39}Ar (E-15 mol)	% ^{39}Ar released	$^{40}\text{Ar}^*$ %	$^{40}\text{Ar}^*/^{39}\text{Ar}_{\text{K}}$	Age \pm 1 s.d. (Ma)
grain 704								
5000	2.407	0.2026	6.461	0.723	100	17.8	0.4744	4.5 \pm 1.1
grain 705								
5000	2.570	0.0538	6.480	1.46	100	23.3	0.6225	5.9 \pm 1.0
718-560 muscovite (J = 0.005235) grain 487								
160	7.031	0.0096	1.755	2.51	44.5	89.5	6.477	61.4 \pm 0.6
5000	10.43	0.0109	13.61	3.14	100	60.1	6.370	60.4 \pm 0.7
total gas age = 60.8								
grain 489								
5000	41.32	0.0103	1.320	4.10	100	98.6	40.87	356.5 \pm 3.3
grain 490								
5000	3.094	0.0150	1.301	3.54	100	81.0	2.674	25.6 \pm 0.4
grain 491								
5000	1.463	0.0163	1.598	3.11	100	58.6	0.9563	9.2 \pm 0.3
grain 492								
5000	2.480	0.0438	3.095	0.609	100	43.7	1.532	14.7 \pm 1.1
grain 493								
5000	1.707	0.0011	0.4051	12.9	100	88.1	1.551	14.9 \pm 0.2
grain 494								
5000	1.967	0.0186	1.493	3.11	100	69.9	1.491	14.3 \pm 0.3
grain 693								
5000	2.431	0.0517	3.742	1.48	100	50.8	1.292	12.2 \pm 0.6
grain 694								
85	5.070	0.4647	11.01	0.295	2.20	32.7	1.809	17.0 \pm 3.2
150	2.629	0.0650	2.984	1.16	10.8	60.1	1.716	16.1 \pm 0.8
5000	2.710	0.0115	0.5187	12.0	100	92.6	2.521	23.7 \pm 0.4
total gas age = 22.9								
grain 697								
5000	1.882	0.1549	1.575	1.30	100	68.3	1.390	13.1 \pm 0.2
718-760 muscovite (J = 0.005289) grain 649								
100	2.548	0.0367	1.432	3.24	54.6	78.4	2.091	19.8 \pm 0.2
150	2.299	0.0950	2.558	1.22	75.2	59.6	1.513	14.4 \pm 1.0
300	2.283	0.0561	3.539	1.10	93.6	45.7	1.205	11.5 \pm 0.9
5000	2.617	0.3070	3.267	0.380	100	47.0	1.635	15.5 \pm 1.3
total gas age = 16.9								
grain 652								
5000	2.805	0.0039	0.4140	9.20	100	93.2	2.647	25.1 \pm 0.3
grain 653								
5000	2.341	0.0874	3.568	1.74	100	50.1	1.256	11.9 \pm 0.9
grain 657								
5000	2.568	0.0650	2.462	1.40	100	64.1	1.809	17.2 \pm 1.0
grain 658								
5000	5.166	0.0180	1.674	3.92	100	88.3	4.636	43.7 \pm 0.7
grain 659								
5000	2.439	0.0214	1.361	4.10	100	79.3	2.002	19.0 \pm 0.5
grain 660								
5000	2.015	0.0197	1.166	3.58	100	76.8	1.635	15.5 \pm 0.2
grain 661								
5000	3.021	0.0327	1.718	3.56	100	79.8	2.479	23.5 \pm 0.4
grain 662								
5000	3.303	0.0643	3.443	1.48	100	65.3	2.254	21.4 \pm 0.9

Table 3 (continued).

Power (mW)	$^{40}\text{Ar}/^{39}\text{Ar}$	$^{37}\text{Ar}/^{39}\text{Ar}$	$^{36}\text{Ar}/^{39}\text{Ar}$ (E-3)	^{39}Ar (E-15 mol)	% ^{39}Ar released	$^{40}\text{Ar}^*$ %	$^{40}\text{Ar}^*/^{39}\text{Ar}_K$	Age \pm 1 s.d. (Ma)
grain 663								
5000	3.104	0.0347	2.419	1.62	100	72.4	2.356	22.3 \pm 0.8
grain 664								
5000	2.569	0.0353	3.505	2.63	100	55.9	1.500	14.3 \pm 0.9
grain 665								
5000	4.168	0.0823	7.585	1.58	100	43.3	1.896	18.0 \pm 0.7

10 to 14 Ma may indicate that the rocks in the Himalayas that reached the surface at that time have been completely removed to the Bay of Bengal and replaced on land with rocks that have cooling ages in the range 10 to 3 Ma. Pb, Nd, and O isotopic analyses of detrital material from Sites 717 and 718 also suggest that the sediment of the Bengal Fan comes from between the MBT and the crest of the Himalayas (Bouquillon et al., this volume). Although K-feldspars with cooling ages in the range 8 to 4 Ma have also been observed in mylonite zones associated with a north-south graben in southern Tibet (Copeland et al., 1989), such material is probably largely held in these grabens and is not a significant component of the Bengal Fan.

A growing body of evidence indicates that the southern margin of the Tibetan Plateau was a significant topographic feature by 20 Ma and since then it has continued to be uplifted and eroded in spatially and temporally discontinuous events (e.g., Copeland et al., 1987a, b; Zeitler, 1985). The episodic nature of the erosional events indicated by these results are consistent with the analysis of Price (1973) who pointed out that the apparent mechanical difficulties of moving entire mountain ranges at one time over large thrusts are easily overcome by many small displacements. Our data are inconsistent with models in which the Himalayas and southern Tibetan Plateau are uplifted either uniformly within the past 40 or predominantly within the past 2 to 5 m.y. (e.g., Zhao and Morgan, 1985, 1987; Zhao and Yuen, 1987; Powell, 1986). The timing of the onset of the uplift and crustal thickening of other parts of the Tibetan Plateau remains uncertain.

CONCLUSIONS

1. Stratigraphic thicknesses within the Bengal Fan appear to be directly related to tectonics in the source area.
2. Pulses of rapid uplift (greater than 1, perhaps as high as 10 mm/yr) have occurred in many locations in the Himalayas and southern Tibetan Plateau for brief spans of time over the last 18 m.y.
3. The southern margin of the Tibetan Plateau has been a significant topographic feature since 18 Ma.

ACKNOWLEDGMENTS

We thank Jim Cochran for introducing us to the Leg 116 data, Jeff Corrigan for providing these samples, Brent Dalrymple for valuable advice while commissioning our laser system, Bill Kidd, John Delano, and David Foster for helpful discussions during data acquisition, and Kip Hodges for discussion of these results. This manuscript was improved by critical comments by Jeff Corrigan, Kevin Crowley, Bill Kidd, Ed Geary, Kevin Burke, and two anonymous reviewers. This research was supported by National Science Foundation grant EAR 8721026 awarded to W.S.F. Kidd, and Department of Energy grant DE-ACO2-82ER13013 awarded to T. M. Harrison.

REFERENCES

- Cochran, J.R., Stow, D.A.V., et al., 1989. *Proc. ODP, Init. Results*, 116: College Station, TX (Ocean Drilling Program).
- Copeland, P., 1990. Cenozoic tectonic history of the southern Tibetan plateau and eastern Himalayas: evidence from $^{40}\text{Ar}/^{39}\text{Ar}$ dating [Ph.D. dissert.]. State Univ. New York at Albany, Albany, NY.
- Copeland, P., Harrison, T. M., Burchfiel, B. C., Hodges K. V., and Kidd, W.S.F., 1987b. Constraints on the age of normal faulting, north face of Mt. Everest: implications for rapid Oligo-Miocene uplift. *EOS*, 68:1444.
- Copeland, P., Harrison, T. M., Kidd, W.S.F., Ronghua, X., and Yuquan, Z., 1987a. Rapid early Miocene acceleration of uplift in the Gangdese Belt, Xizung (southern Tibet) and its bearing on accommodation mechanisms of the India-Asia collision. *Earth Planet. Sci. Lett.*, 86:240-252.
- Copeland, P., Kidd, W.S.F., Harrison, T. M., Yun, P., Bingshwen, Z., Yuquan, Z., and Xie, Y., 1989. Uplift of the Nyainqentanghla and the crustal thickening history of southern Tibet. *EOS*, 70:1372.
- Coulon, C., Maluski, H., Bollinger, C., and Wang, S., 1986. Mesozoic and Cenozoic volcanics from central and southern Tibet: ^{39}Ar - ^{40}Ar dating, petrological characteristics and geodynamical significance. *Earth Planet. Sci. Lett.*, 79:281-302.
- Curry, J. R., and Moore, D. G., 1971. Growth of the Bengal deep-sea fan and denudation in the Himalayas. *Geol. Soc. Am. Bull.*, 82:563-572.
- Dalrymple, G. B., and Duffield, W. A., 1988. High precision $^{40}\text{Ar}/^{39}\text{Ar}$ dating of Oligocene rhyolites from the Mogollon-Datil volcanic field using a continuous laser system. *Geophys. Res. Lett.*, 15:463-466.
- Deino, A. L., 1989. Single-crystal $^{40}\text{Ar}/^{39}\text{Ar}$ dating as an aide in correlation of ash flows: examples from the chimney Spring/New Pass Tuffs and the Nine Hill/Bates Mountain Tuffs of California and Nevada. *Continental Magmatism Abstracts, IAVCEI General Assembly*. New Mexico Bur. Mines Mineral Res. Bull., 131:70.
- Dewey, J. F., and Burke, K.C.A., 1973. Tibetan, Variscan and Precambrian basement reactivation: products of continental collision. *J. Geol.*, 81:683-692.
- Ferrara, G., Lombardo, B., Tonarini, S., 1983. Rb/Sr geochronology of granites and gneisses from the Mount Everest region, Nepal Himalayas. *Geol. Rundsch.*, 72:119-136.
- Foland, K. A., 1974. ^{40}Ar diffusion in homogenous orthoclase and an interpretation of Ar diffusion in K-feldspar. *Geochim. Cosmochim. Acta*, 38:151-166.
- Govindaraju, K., 1979. Report (1968-1978) on Two mica reference samples: biotite Mica-Fe and Phlogopite Mica-Mg. *Geostand. Newsl.*, 3:3-24.
- Harrison, T. M., Armstrong, R. L., Naeser, C. W., and Harakal, J. E., 1979. Geochronology and thermal history of the Coast Plutonic Complex, near Prince Rupert, B.C. *Can. J. Earth Sci.*, 16:400-410.
- Harrison, T. M., Copeland, P., Hodges, K. V., Le Fort, P., and Pêcher, A., 1989. A late Miocene thermal perturbation along the MCT related to movement on the MBT: recurring tectonothermal consequences of collision. *Eos*, 70:1380.
- Harrison, T. M., and Fitz Gerald, J. D., 1986. Exsolution in hornblende and its consequences for $^{40}\text{Ar}/^{39}\text{Ar}$ age spectra and closure temperature. *Geochim. Cosmochim. Acta*, 50:247-253.

- Harrison, T. M., and McDougall, I., 1981. Excess ^{40}Ar in metamorphic rocks from Broken Hill, New South Wales: implications for $^{40}\text{Ar}/^{39}\text{Ar}$ age spectra and the thermal history of the area. *Earth Planet. Sci. Lett.*, 55:123–149.
- Harrison, T. M., and McDougall, I., 1982. The thermal significance of potassium feldspar K-Ar ages inferred from $^{40}\text{Ar}/^{39}\text{Ar}$ age spectrum results. *Geochim. Cosmochim. Acta*, 46:1811–1820.
- Ingersoll, R. V., Suczek, C. A., 1979. Petrology and provenance of Neogene sand from Nicobar and Bengal Fans, DSDP Sites 211 and 218. *J. Sediment. Petrol.*, 49:1217–1228.
- Kai, K., 1981. Rb-Sr ages of the biotite and muscovite of the Himalayas, eastern Nepal: its implication in the uplift history. *Geochem. J.*, 15:63–68.
- Le Fort, P., 1989. The Himalayan orogenic segment. In Sengör, A.M.C. (Ed.), *Tectonic Evolution of the Tethyan Regions*. NATO ASI Ser., Ser. C, 259:289–386.
- LoBello, Ph., Feraud, G., Hall, C. M., York, D., Lavina, P., and Bemat, M., 1987. $^{40}\text{Ar}/^{39}\text{Ar}$ step heating and laser fusion dating of a Quaternary volcano from Neschers, Massif Central, France: the defeat xenocrystic contamination. *Isot. Geosci.*, 66:61–71.
- Lovera, O. M., Richter, F. M., and Harrison, T. M., 1989. $^{40}\text{Ar}/^{39}\text{Ar}$ geothermometry for slowly cooled samples having a distribution of diffusion domain sizes. *J. Geophys. Res.*, 94:17917–17935.
- Maluski, H., Matte, P., and Brunel, M., 1988. Argon 39—Argon 40 dating of metamorphic and plutonic events in the North and High Himalayas belts. *Tectonics*, 7:299–326.
- McDougall, I., and Harrison, T. M., 1988. *Geochronology and Thermochronology by the $^{40}\text{Ar}/^{39}\text{Ar}$ Method*. Oxford Monogr. Geol. Geophys., 9.
- Molnar, P., 1984. Structure and tectonics of the Himalayas: constraints and implications of geophysical data. *Annu. Rev. Earth Planet. Sci.*, 12:489–518.
- Moore, D. G., Curray, J. R., Raitt, R. W., and Emmel, F. J., 1974. Stratigraphic-seismic section correlation and implications to Bengal Fan history. In von der Borch, C. C., Sclater, J. G., et al., *Init. Repts. DSDP*, 22: Washington (U.S. Govt. Printing Office), 403–412.
- Powell, C. McA., and Conaghan, P. J., 1973. Plate tectonics and the Himalayas. *Earth Planet. Sci. Lett.*, 20:1–12.
- Powell, C. McA., 1986. Continental underplating model for the rise of the Tibetan Plateau. *Earth Planet. Sci. Lett.*, 81:79–94.
- Price, R. A., 1973. The mechanical paradox of large overthrusts. *Geol. Soc. Am. Abstr. Programs*, 5:772.
- Purdy, J. W., and Jäger, E., 1976. K-Ar ages on rock-forming minerals from the Central Alps. *Mem. Inst. Geol. Min. Univ. Padova*, 30.
- Rabinowitz, P. D., Dipiazza, N., and Matthias, P. K., 1988. Isopach map of sediments in the Indian Ocean. AAPG.
- Robbins, G. A., 1972. Radiogenic argon diffusion in muscovite under hydrothermal conditions [M.S. thesis]. Brown Univ., Providence.
- Wagner, G. A., Reimer, G. M., and Jäger, E., 1977. Cooling age derived by apatite fission-track, mica, Rb-Sr and K-Ar dating: the uplift and cooling history of the Central Alps. *Mem. Inst. Geol., Univ. Padova*, 30.
- Zeitler, P. K., 1985. Cooling history of the NW Himalayas. *Tectonics*, 4:127–151.
- Zeitler, P. K., and Fitz Gerald, J. D., 1986. Saddle-shaped $^{40}\text{Ar}/^{39}\text{Ar}$ age spectra from young, microstructurally complex potassium-feldspars. *Geochim. Cosmochim. Acta*, 50:1185–1199.
- Zeitler, P., Johnson, N. M., Briggs, N. D., and Naeser, C. W., 1986. Uplift history of the NW Himalayas as recorded by fission-track ages on detrital Siwalik zircons. In Jinqing H. (Ed.), *Proc. Symp. Mesozoic Cenozoic Geol.*: Beijing (Geol. Publ. House), 481–494.
- Zhao, W., and Morgan, W. J., 1985. Uplift of the Tibetan plateau. *Tectonics*, 4:359–369.
- Zhao, W., and Morgan, W. J., 1987. Injection of Indian crust into Tibetan lower crust: a two-dimensional finite element model study. *Tectonics*, 6:489–504.
- Zhao, W., and Yuen, D. A., 1987. Injection of Indian crust into Tibetan lower crust: a temperature-dependant viscous model. *Tectonics*, 6:505–514.

Date of initial receipt: 9 March 1989

Date of acceptance: 22 January 1990

Ms 116B-119

Table 4. $^{40}\text{Ar}/^{39}\text{Ar}$ total fusion results from multigrain separates of muscovite and muscovite from samples at Sites 717 and 718.

Temp °C	$^{40}\text{Ar}/^{39}\text{Ar}$	$^{37}\text{Ar}/^{39}\text{Ar}$	$^{36}\text{Ar}/^{39}\text{Ar}$ (E-3)	^{39}Ar (E-13 mol)	% ^{39}Ar released	$^{40}\text{Ar}^*$ %	$^{40}\text{Ar}^*/^{39}\text{Ar}_K$	Age \pm 1 s.d. (Ma)
717-220 K-feldspar total fusion (J = 0.005329; wt. = 25.50 mg)								
1540	7.955	0.0184	2.152	46.6	100	91.3	7.285	68.7 \pm 0.1
717-520 K-feldspar total fusion (J = 0.005351; wt. = 26.01 mg)								
1540	8.552	0.0180	1.730	46.8	100	93.6	8.006	75.7 \pm 0.1
718-560 K-feldspar total fusion (J = 0.005329; wt. = 27.51 mg)								
1540	8.106	0.0116	1.641	49.4	100	93.4	7.586	71.5 \pm 0.1
718-660 K-feldspar total fusion (J = 0.005305; wt. = 19.78 mg)								
1540	12.71	0.0197	2.584	36.0	100	93.5	11.91	110.5 \pm 0.3
717-220 muscovite total fusion (J = 0.005354; wt. = 18.29 mg)								
1450	3.946	0.0568	1.765	25.0	100	85.9	3.393	32.5 \pm 0.1
717-520 muscovite total fusion (J = 0.005222; wt. = 21.15 mg)								
1450	3.437	0.0025	1.497	31.5	100	85.3	2.959	27.7 \pm 0.1

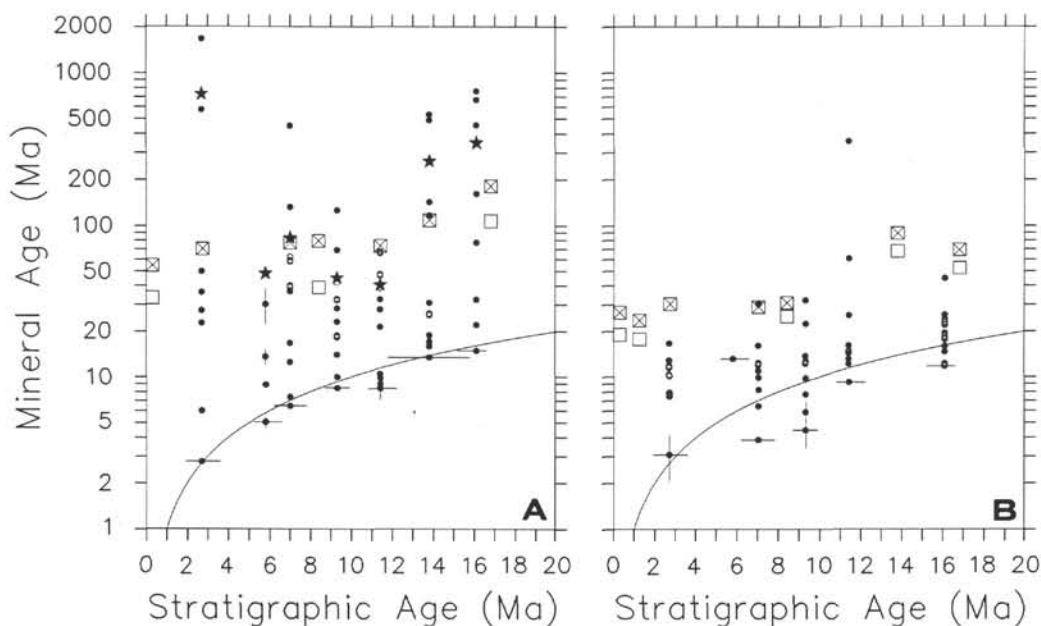


Figure 10. Semi-log plot of $^{40}\text{Ar}/^{39}\text{Ar}$ mineral age vs. stratigraphic age: **A.** K-feldspars, **B.** Muscovites. Circles represent minimum age on age spectrum or total fusion age where only one step was performed for single-crystal analyses. Open squares represent minimum ages on age spectra from multigrain separates. Squares with X's are total fusion ages of multigrain separates. Stars represent weighted average of single crystal analyses from one stratigraphic interval. Uncertainties on mineral age are less than size of symbols, except where shown. Uncertainties on stratigraphic age are shown only for the sample with the youngest apparent mineral age from each stratigraphic level. For ease of representation, we have chosen to treat all grains from a particular interval as if they came from the midpoint of the interval with an uncertainty that encompasses the uncertainties in the ages of the top and bottom of the interval; these uncertainties vary, so that some data appear to be plotted away from the midpoint.

Table 5. Summary of $^{40}\text{Ar}/^{39}\text{Ar}$ ages (Ma) from muscovite and muscovite from samples at Sites 717 and 718.

Stratigraphic interval (mineral)	Bulk separate total fusion	Single-crystal weighted average	Bulk separate minimum age	Single-crystal minimum age
717-0 KF	54.3		33.2	
717-220 KF	68.7	727		2.8
717-420 KF		48.4		5.1
717-520 KF	75.7	83.0		6.4
717-720 KF		45.1		9.1
718-290 KF	79.2		39.0	
718-560 KF	71.5	40.6		8.0
718-660 KF	111	264		13.4
718-760 KF		349		14.9
718-860 KF	183		107	
717-0 MUSC	26.7		19.1	
717-120 MUSC	23.4		16.8	
717-220 MUSC	32.4	10.6		3.1
717-520 MUSC	27.7	12.2		3.9
717-720 MUSC		16.6		4.5
718-290 MUSC	30.8		24.4	
718-560 MUSC		51.0		9.2
718-660 MUSC	88.2		69.7	
718-760 MUSC		22.0		11.5
718-860 MUSC	69.6		53.1	

KF = K-feldspar, MUSC = muscovite

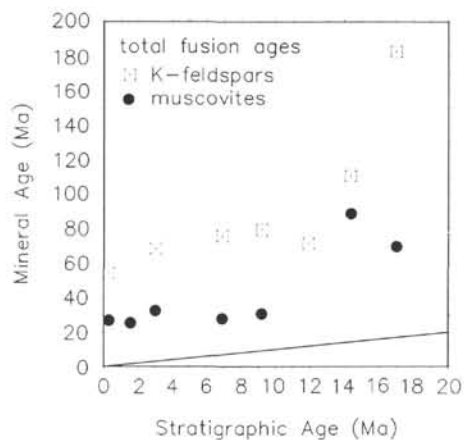


Figure 11. Linear plot of total fusion ages for bulk separates vs. stratigraphic age.